NTNU
Norwegian University of Science and Technology
Faculty of Information Technology and Electrical Engineering
Department of Electric Power Engineering

Martin Sanden

Investigation of Contact Erosion and Arc-Welding in a Medium Voltage Switching Device Using COMSOL

Master's thesis in Energy and the Environment
Supervisor: Kaveh Niayesh, IEL
June 2019

NTNU
Norwegian University of
Science and Technology

Martin Sanden

Investigation of Contact Erosion and Arc-Welding in a Medium Voltage Switching Device Using COMSOL

Master's thesis in Energy and the Environment
Supervisor: Kaveh Niayesh, IEL
June 2019

Norwegian University of Science and Technology
Faculty of Information Technology and Electrical Engineering
Department of Electric Power Engineering

NTNU
Norwegian University of
Science and Technology

Problem Description

A basic model of deformed mesh on a medium voltage contact has previously been examined, where arcing resulted in evaporation of contact materials.

In this master's thesis, a basic model for the material transport in medium voltage contacts during closing will be developed. Two contacts will be examined, a fixed and a moving contact, making it necessary to implement a moving mesh. In addition, phase change from solid to liquid state is included. For this purpose, the multi-physics simulation tool, COMSOL, will be used.

The main goals of this master's thesis is to examine the influence pre-strike arc has on the contacts during closing operation. Further, the aims is to investigate the welding behaviour of the closing contacts, and study the contact erosion at different short-circuit currents and arcing times.

Abstract

This master's thesis addressed the effect pre-strike arc had on a medium-voltage switching devices during making operation. The main aims were to find the amount of contact erosion and arc-weld strength after the making operation had occurred.

Three base models were developed in COMSOL. One for each contact material simulated: copper, tungsten and copper-tungsten. Each base model consisted of a fixed and a moving contact. The changing parameters were the short-circuit current and the arcing time.

It was found that pure copper had the lowest strength toward contact erosion and arc-welding. Additionally, the results showed that copper-tungsten tolerated these thermal stresses best. At maximum short-circuit current and arcing time, the contact erosion for the contact materials copper, tungsten and copper-tungsten were 26.88 mg, 17.37 mg and 15.45 mg, respectively.

The contact material copper-tungsten were further examined, to see the impacts material distribution had on contact erosion and arc welding. The results showed that the contact material with high tungsten density performed the best.

Altogether, when examining copper-tungsten, it was found that increasing the amount of tungsten particles present at the contacts, reduced both contact erosion and arc welding strength. These results indicates that the contact material copper-tungsten is good with regards to thermal stresses during making operations.

Abstract (Norwegian)

Denne master oppgaven omhandler effektene lysbuen hadde på en mellomspennings effektbryter under lukkeoperasjoner. Hovedmålet for oppgaven var å finne den totale kontakterosjonen og styrken på lysbuesveisen etter at lukking hadde inntruffet.

Tre grunnmodeller ble laget i simuleringsprogrammet COMSOL. En for hver kontakt material undersøkt: kobber, wolfram og komposittmaterialet kobber-wolfram. Hver grunnmodell besto av en fast og en bevegelig elektrode. De endrede parameterne undersøkt, var kortslutningsstrømmen og aktiv lysbuetid.

Det ble funnet at ren kobber hadde den laveste styrken i forhold til kontakterosjon og lysbuesveising. I tillegg, viste resultatene at kobber-wolfram tolererte termiske belastinger best. Ved maksimum kortslutningsstrøm og lysbuetid ble det observert kontakterosjon på henholdsvis 26.88 mg, 17.37 mg og 15.45 mg for kobber, wolfram og kopper-wolfram.
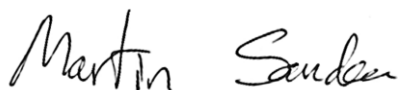
Kontaktmaterialet kobber-wolfram ble videre undersøkt for å se på innvirkningen materialdistribusjon hadde på kontakterosjon og lysbuesveising. Resultatene viste at kontaktmaterialet med høyt innhold av wolfram, presterte best.

Kort oppsummert viser undersøkelsen av kontaktmaterialet kobber-wolfram at en økning av wolfram partikler i elektrodene, reduserte kontakterosjon og styrken på lysbuesveisen. Resultatene indikerte at kontaktmaterialet kobber-wolfram fungerer godt med tanke på termiske belastinger under lukkeoperasjoner.

Preface

This master's thesis was written during the spring semester of 2019. This is the final part of the two-year master program in Energy and the Environment at the Norwegian University of Science and Technology. The thesis is carried out at the Department of Electric Power Engineering. The project work has mostly been literature search, with numerous hours spent in the simulation program COMSOL Multiphysics.

This master's thesis is a continuation of my project report about contact erosion of a medium voltage switching device. The focus is now directed at the making operation where both contact erosion and arc welding is the main aims.

Martin Sanden

25. June 2019

Acknowledgement

I wish to thank my supervisor, Professor Kaveh Niayesh for sharing all his knowledge, making me able to carry out this work. I sincerely appreciate all the time you have spent supervising me throughout the last year. Your doors were always open, when I had questions. Thank you for all the help and knowledge that you have given me.

I would like to thank Milad Mohammadhosein for his extraordinary help during my specialisation project. Your help with simulations and literature search have been priceless.

I wish to thank Ali Kadivar for his extremely good understanding of COMSOL. Your wise words and tips made me think differently, when simulating in COMSOL. Without your tips in COMSOL, the simulations in this master's thesis would not have been possible to conduct.

I wish to thank my family for supporting me throughout my education. All of you have always been there to support me through good and bad times. Your kind words have motivated me and made me work harder to achieve my goals. Thank you, I would not be able to deliver this master's thesis today without all your support.

Last but not least, I will thank my older sister Mai-Linn Sanden and my beloved Lydia Brunvoll Sandøy for your help and support. You have always been there if I needed help and your wise words have guided me through my education. Every time I need help, I can always count on you. Your feedback and constructive criticism on this master's thesis have been invaluable. I express my sincerest gratitude for all the time you have invested in this project. Both of you have a special place in my heart.

x

Content List

Chapter 1

Introduction

1.1 Motivation

Electrical switching devices are one of the most important components in the electrical system. They are responsible for the protection of electrical components and other vital parts of the electrical system. In addition, they are able to control power flow to different subsystems and components. There are four types of electrical switches; circuit breakers, dis-connectors, load breakers and earthing switches. Switching devices are making and breaking load and short circuit currents, implying that a switching device should be able to change its impedance from almost zero (closed position) to almost infinitely (open position) [1].

In modern power systems, renewable energy continues to have an increased market share. Consequently, stability and flexibility are the most essentials factors to take into consideration. During every switching operation (i.e. opening or closing) the device is exposed for high mechanical and electrical stresses, causing the operating mechanism to be influenced. Two of these factors are contact erosion and arc-welding [2].

Contact erosion is considered as material transportation where the contact material changes its properties and geometrical shape. During switching operation an arc ignites causing the contact material to evaporate. Evaporation causes some contact material to leave the contact and disappear out to the surroundings. Contact erosion is one of the main factors for determining the life time of a switchgear. If the contact erosion becomes substantial, causing unwanted stresses, the switchgear must be repaired before it can continue to operate.

Arc-welding is considered as a continuous mechanical contact between the contacts. During making operation, the contact material melts due to the heat dissipated from the pre-strike arc. When the contact mechanically touches, the molten part fuses together and creates a weld between the contacts. Excessive arc welding at the contact surface can prevent the switchgear to respond to the next opening command. Consequently, the opening mechanism does not produce sufficient force to break all the welding point holding the contact together [1].

Therefore, understanding and examination the contact behaviour during and after arcing are crucial for preventing future failures for switching devices. A switching device should always be reliable, e.g. it should open when commanded (dependable) and stay closed otherwise (secure). Without a functioning switching device, the outcome can both be dangerous and expensive [2].

1.2 Software Used in this Master's Thesis

Simulations and calculations have been performed in COMSOL Multiphysics®. Different types of physical objects can be simulated in COMSOL e.g. electrical, mechanical, thermal, fluid flow. This master's thesis uses physics:

- *"Heat transfer in liquids – simulate heat transportation inside the simulated model."*
- *"Deformed geometry – simulate the deformation and the movement of the model."*

All figures presented in this master's thesis is exported directly from the simulations or made in Microsoft PowerPoint. The graphs presented in chapter 5 *"Results from the Simulations",* are created in Microsoft Excel. All the data are imported from COMSOL, modified and presented.

1.3 Structure of the Thesis

Chapter 1 - Introduction, describes the motivation to conduct this master's thesis. Followed by a brief presentation of the programs used in this master's thesis.

Chapter 2 – Summary of the specialisation project, summarizes the specialisation project with focus on the methodology and key findings. Further, the most relevant literature from the specialisation project is presented. It finishes with the measures done to transit the specialisation project into the master's thesis.

Chapter 3 – Theory and Literature Review, explains the requirements, stresses and making- and breaking capacity of switching equipment. Further, the theory behind the breakdown mechanisms during making operation for both gas-filled and vacuum breakers are described. This chapter finishes with the explanation and concerns of contact welding.

Chapter 4 – Modelling of the System Using COMSOL Multiphysics®, describes the modelling part in COMSOL. This chapter includes the necessary information to produce the simulations in this master's thesis.

Chapter 5 – Results from the Simulations, presents the results produced in this master's thesis. There is conducted three main simulations: contact erosion, weld strength and material distribution.

Chapter 6 – Discussion, presents a reflection of the results generated from the simulations. Four main points are discussed in this chapter.

Chapter 7 – Conclusion, includes the most important findings found in the master thesis.

Chapter 8 – Further Work, presents some suggestions that can be included in the COMSOL model to increase its validity.

Chapter 2

Summary of the Specialisation Project

This master's thesis is based on the concepts and methods done in the specialisation project last semester. Thereby, it is essential to summarise the literature search, key methods and findings to give the reader an understanding of the concepts used in this master's thesis. This chapter presents a short summary of the specialisation project, followed by a summary of some of the theoretical mechanisms used in this master's thesis. The chapter ends with the new implementations in order to change the main focus towards making operation.

2.1 Summary of the Specialisation Project

The project report addressed the problem of erosion on a medium-voltage switching device during breaking operation. The aim of the project was to examine the influence the electrical arc had on the contact material. A basic model of material transportation was developed to investigate the erosion rate of contacts during arcing. The simulations were performed in COMSOL Multiphysics®. Three different models were made to examine [2]:

i. Temperature distribution in the electrode during breaking.
ii. Impact the generated heat had on the electrode, where geometrical deformation was implemented.
   The dependency between current level and the amount of lost material.

The first simulation examined the temperature distribution inside the contact material without any deformation. The second simulation resulted in a decrease in the contact material volume and mass. This simulation made it possible to examine the amount of lost material during breaking operation. For the third simulation, the short circuit current varied between 5 kA to 25 kA (rms value). The purpose was to find the influence different short-circuit currents had on the contact surface [2].

For simplicity, erosion was modelled with a material phase shift directly from solid- to gaseous phase. Normally, a metal transfers from solid- to liquid phase and from liquid- to gaseous phase. The liquid phase was neglected in order to reduce the complexity of the simulations. The materials examined in the project were copper (Cu), Tungsten (W) and the composite material copper-tungsten (CuW) [2].

Simulation was made as simple as possible without influencing the validity of the results. Some assumptions were made to make the simulations simpler.

i.   The electrical arc was converted into a heat source due to its complexity. The heat source was assumed to be divided equal between the electrodes making it possible to only examine one of the electrodes.

ii.   Geometrical dimensions were held constant for every simulation. Making it possible to compare the results between the simulations. Each simulation was performed for all three contact materials.

iii. There was no cooling implemented in the simulations. Thus, all the generated heat went directly towards the electrodes causing *"the worst-case scenario"* for the contact material.

iv.   The voltage drop was held constant throughout the entire simulation [2].

The results indicated that the losses were significantly lower for the composition material copper-tungsten, compared to contact material consisting of pure copper or tungsten. This implies that the effects of having a combination with a conductive and a refractory material increased the erosion rate of the contact material. Additionally, the results showed that the weakest contact occurred when the contact material consisted of pure copper. This is directly connected with the thermal properties of copper, i.e. the low evaporation temperature and the low thermal capacity [2].

6

2.2 Short Literature Summary of the Specialisation Project

2.2.1 Materials Used in Switching Devices

A circuit breaker is required to withstand all kind of stresses present during normal and abnormal conditions. It should be able to conduct any current without generating any heat when in the closed position, open the breaker (break any current) at any given time and close the breaker (make any current) after a fault has been cleared. This implies that the contact material is a vital part of a switching device and has to fulfil all requirements mentioned. The desired properties of breakers are [2] - [4]:

   i.   Low contact resistance to prevent generation of heat.

  ii.   Low arc erosion to prevent the contact material evaporation during operation.

 iii.   High resistance towards melting and arc welding, to prevent contact surface to get welded together during making operation.

 iv.   Low heat expansion coefficient to prevent material expansion when the material is heated up.

Generally, the electrodes are made of two types of material. The first material is a conductive metal used to increase the electrical and thermal conductivity and decrease the contact resistance. Typical conductive materials are copper (Cu) and silver (Ag), since they have extremely good electrical properties compared to other metals. Additionally, they have high thermal conductivity causing them to conduct heat away relatively fast. The other group is the refractory metals. These materials have an extraordinary resistance towards heat and wear. Typical refractory materials are tungsten (W), carbon (C) and molybdenum (Mo), since their melting point is extremely high compared to other metals. Furthermore, they increase the mechanical strength of the contact, decrease the contact wear and prevents arc welding of the contacts [2], [5].

The most commonly used contact materials in power switching devices are; silver-tungsten (AgW), silver-tungsten carbide (AgWC) and copper-tungsten (CuW). The advantages and disadvantages with these materials are presented in Table 1 [2], [5].

Table 1: Advantages and disadvantages for the composite materials silver-tungsten (AgW), silver-tungsten carbide (AgWC), and copper-tungsten (CuW).

Contact material	Advantages	Disadvantages
Silver-Tungsten	▪ Good conducting properties from silver. ▪ Good mechanical and electrical wear withstand of tungsten. ▪ Possible to get in the range 10% to 90% silver, making it possible to form the contact material for different operation purposes.	▪ Expensive due to price of silver. ▪ High content of silver increases the chance of erosion and arc welding. ▪ Silver have lower melting and boiling point than copper.
Silver-Tungsten Carbide	▪ Harder material than silver-tungsten. ▪ Better abilities towards arc erosion and contact wear than silver-tungsten.	▪ Decreased current carrying and thermal abilities, causing more generation of heat and stresses.
Copper-Tungsten	▪ Cheaper alternative than silver-tungsten. ▪ Good substitute material for silver-tungsten and it almost has the same properties.	▪ Low resistance from oxidation. ▪ Copper have lower conducting abilities than silver.

The specialisation project and the master's thesis focus on the three types of materials; copper, tungsten and the composite material copper-tungsten. It is impossible to produce copper-tungsten as a continuous phase, as for an alloy, because the melting temperature for copper is lower than tungsten.

Powder metallurgy is the only method to produce the composition material copper-tungsten. Powder metallurgy is a method where copper and tungsten powder are blended together, sintered and shaped into the desirable geometry. During the sintering process the ambient temperature must be higher than the melting temperature of copper. This causes the copper particles to melt and fuse together creating a liquid phase around the tungsten atoms. When cooled down the copper phase solidifies, traps the tungsten particles and creates a solid geometry. The effects of the sintering process cause the new material to be divided into material zones. This causes the thermal and electrical properties to be dependent on the material present in the zone. This has been illustrated in Figure 1 [2], [7], [8].
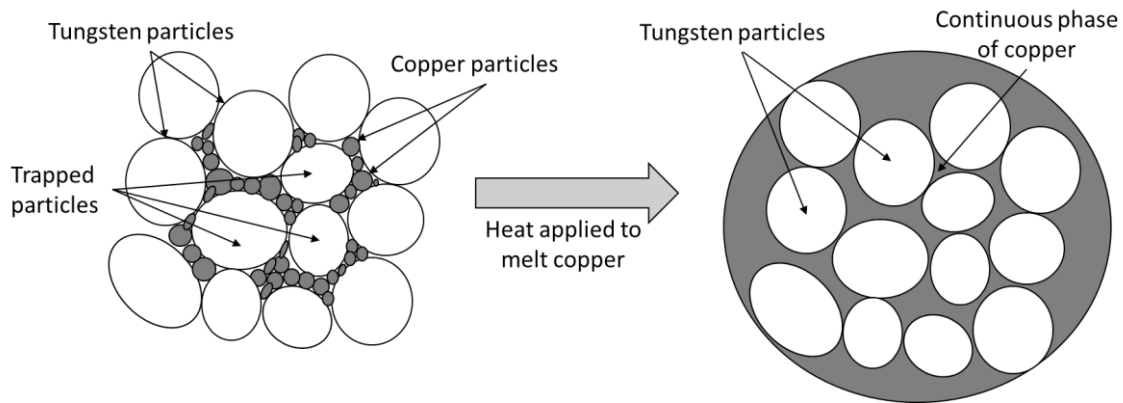
Figure 1: An illustration of a sintered copper-tungsten binding. Copper particles (gray) fuses together and trap tungsten particles (white). This results in a compact material were tungsten particles are surrounded by a continuous phase of copper. The distribution of copper and tungsten varies for each sample created.

2.2.2   Material Loss due to Vaporisation

Materials will at some point experience a phase shift when heat is applied. There are four different material phases; solid, liquid, gas and supercritical plasma. Each phase has its own characteristics and their properties changes with the change in phase. The first of the material phases is the solid phase. Here, particles (ions, atoms and molecules) are closely packed together and have little freedom for movement. It is stable and have a defined geometry and volume. The only way to change its geometrical structure is by applying a force such that the geometry breaks or becomes deformed.

When heated above its melting point, the solid phase becomes liquid. In the liquid phase, the particles are free to move. There is no clearly defined geometry, but the volume remains constant. When applying a force, the shape can easily be changed.

Heating the liquid until its boiling point, transforms it into gas. Now, the particles have enough energy to break free from their bonds, making it possible to move freely. The volume is not defined, and gas has no district shape. Gas fills the available space where it is contained. Gas can easily escape if it is not concealed inside a container.

The last material phase is supercritical plasma. Plasma is achieved by increasing the temperature of gas until the gas molecules becomes ionized. The ionized gas has an increased electrical conductivity due to the increased number of free electrons. It is essential for the insulation medium to be in the plasma state for an electrical arc to be active. Figure 2 illustrates the first three stages of material phase shift.
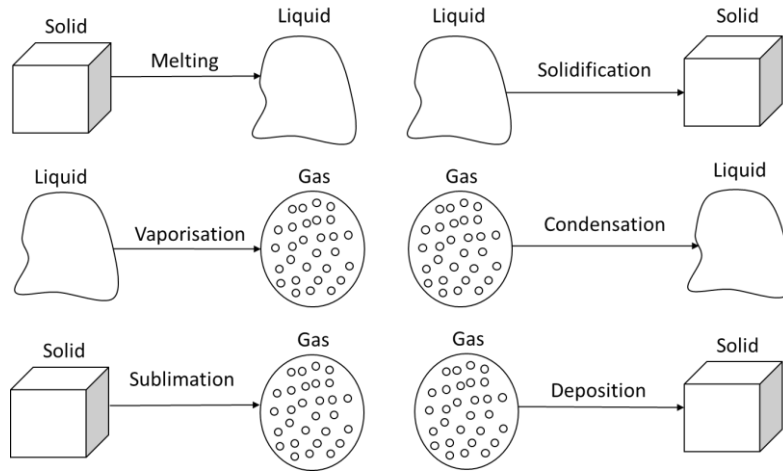
Figure 2: An illustration of the different phase shifts for material. The different phases presented is solid, liquid and gas. The different phase changes have different names depending on the start and end state.

For the object to phase shift, it is necessary to apply heat to the object. The amount of energy depends on the material, shape and temperature. Different molecular bindings need to have different amounts of energy to be split. A general equation for energy needed to transform a solid object to gas is given in Equation (2.1) and presented in Figure 3 [2], [8].

$$\Delta H_{sublimation} = \Delta E_{th(Solid)} + \Delta E_{b(S \to L)} + \Delta E_{th(Liquid)} + \Delta E_{th(L \to G)} + \Delta E_{th(Gas)} \quad (2.1)$$

- $\Delta H_{sublimation}$ Total amount of energy needed to convert an object from the solid state to the gaseous phase.
- $\Delta E_{th(Solid)}$ Amount of energy needed to convert an object from one given temperature and up to its melting point.
- $\Delta E_{b(S \to L)}$ Amount of energy needed to convert the entire object from the solid phase to the liquid phase (with constant temperature).
- $\Delta E_{th(Liquid)}$ Amount of energy needed to convert an object from liquid state until it starts gasifying.
- $\Delta E_{th(L \to G)}$ Amount of energy needed to convert the entire object from the liquid phase to the gaseous phase (with constant temperature).
- $\Delta E_{th(Gas)}$ Amount of energy needed to convert an object from the gaseous state until it starts to self-ionize.
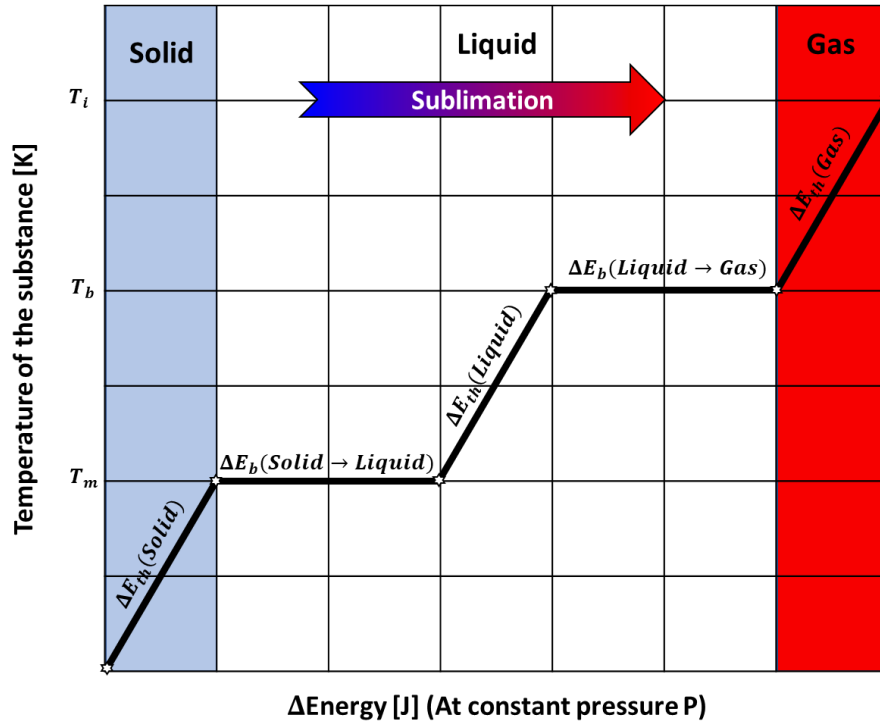
Figure 3: The graph illustrates the energy needed to transform an object from the solid stage to the gaseous phase. The temperatures T_m, T_b and T_i is the melting temperature, boiling temperature and ionization temperature respectively. Blue defines the solid state, white defines the liquid state and red defines the gaseous phase [2], [7].

2.2.3   Arc Gap Voltage – Static Arc

It is common to differentiate between static- and dynamic arcs when inspecting switching arcs. The difference between them is the aspect of time. Static arc can be assumed to not be influenced by the time, i.e. all the parameters are constant if inspecting the arc after all the transient phenomena has disappeared. It is opposite when examining a dynamic arc. For dynamic arcs, current and cooling varies with time. This influences the arc temperature, conductivity and cross-section [1], [2].

In this master's thesis the arc is assumed to be static. The static arc can be divided into three main regions; the anode-, the cathode region and the arc column as illustrated in Figure 4. The voltage drop in the arc mainly occurs close to the electrodes, where the biggest contribution originates from the cathode region. The total voltage drop can be calculated by summarising the voltage drops in each region as presented in Equation (2.2).

$$V_{gap} = V_{cathode} + V_{arc\ column} + V_{anode} \tag{2.2}$$

11
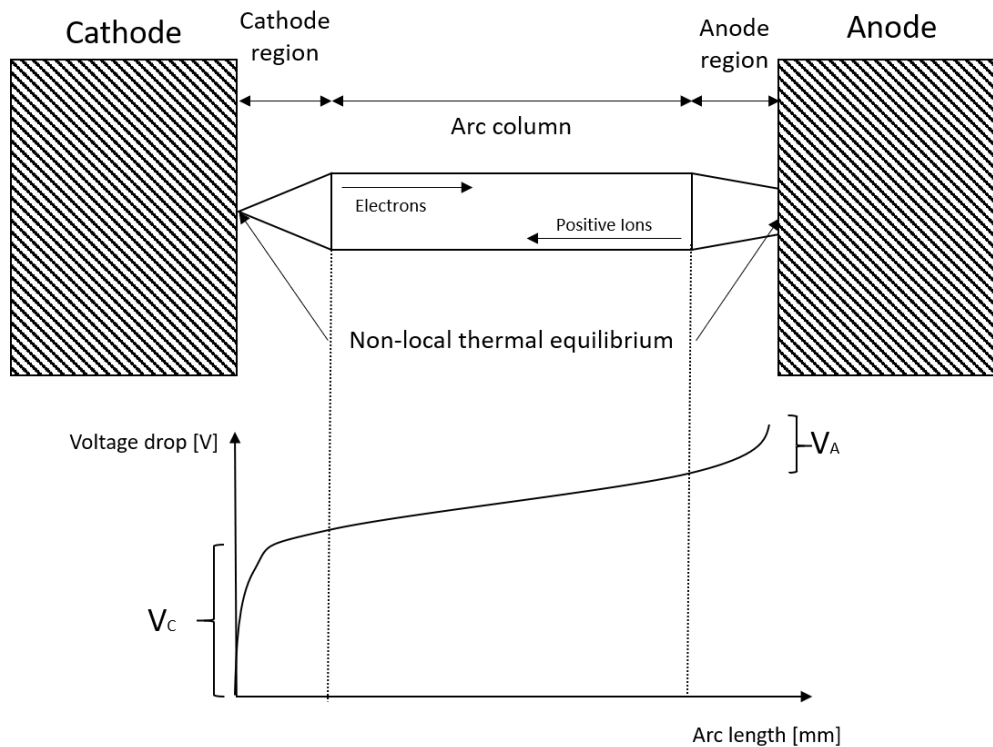
Figure 4: Illustrates the cross-section of a stationary arc. The three zones: anode region, arc column and cathode region has been included. The graph presents the voltage drop as a function of the arc distance. The graph shows that the highest contributor to the voltage drop is from the cathode region [1], [2].

Experiments implies that the voltage drop in a static arc has some general tendencies. The highest voltage drop is observed in the area near the cathode, with a range of 15 V to 20 V. In the anode region the voltage drop decreases to the range of 1 V to 12 V. The value of the voltage drop close to the contact surface heavily depends on current level, pressure and the contact materials. For the arc column, the voltage drop depends on the distance between the contacts. Therefore, the voltage drop changes with time during breaking and making of the current [1], [2].

2.2.4   Temperature Distribution Inside an Arc

Arc temperature strongly depends on the current level, since thermal conductance and cooling changes with variation in current. Experiments implies that low current arcs has a gaussian distribution, where the highest temperature is at the centre of the arc and decays outwards. For low current arcs, temperature, conductivity and cooling are proportional with current, as illustrated in Figure 5 [1], [2].

This effect is not proportion for large current arcs, as the arc cooling exceeds the generation of heat, causing a stable arc temperature. With increasing arc current, the effects of cooling becomes so immense, causing a low variation in temperature and conductivity. Hence, an increase in arc current increases the arc cross-section, as presented in Figure 5 [1], [2].
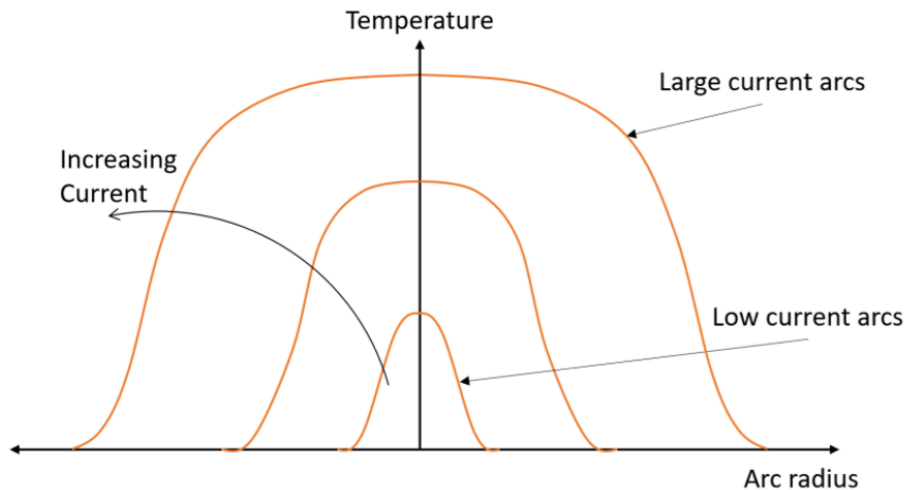
Figure 5: Temperature distribution of an electrical arc with respect to the arc radius. For low currents, an increase in current causes the arc temperature to increase. For large currents, an increase in current causes an increase in the arc cross-section [2].

2.3 Transition from Specialisation Project to Master's Thesis

Some changes have been implemented between the specialisation project and the master's thesis. In the specialisation project, the breaking operation were the main focus of investigation. Where the factors influencing the contact during opening operation were examined. In the master's thesis the main focus of investigation is the making operation.

The COMSOL model created in the specialisation project will be modified for simulation of the closing operation. New implementations improves the old simulation making it more realistic. These features are mentioned below;

Implementing melting/phase change

In the specialisation project, the COMSOL model transformed directly from solid state to gaseous phase (sublimation) when exposed for heat. This was to make the simulation simple and not time consuming. The new implementation to the COMSOL model is to implement the liquid phase. When introducing the melting temperature of the material, the contact material melts when it exceeds this threshold. The new implementation makes the model more realistic, as the thermal properties changes according to the phase of the material. This requires some material properties to be found. These parameters are;

- ρ_L The material density of the metal in the liquid phase $[kg/m^3]$.
- $C_{p,L}$ The heat capacity of the metal in the liquid phase $[J/kg \cdot K]$.
- k_L Heat capacity of the liquid metal $[W/m \cdot K]$.
- L_m Latent heat of melting [kJ/kg], this is the amount of energy (per mass) needed to fully convert a solid substance to a liquid.

These new material properties are assumed to be constant after melting has begun and until it begins to evaporate. In addition, the heat physic used has been changed from *"heat transfer in solids"* to *"heat transfer in liquids".*

Implementing movement to the contact.

In the specialisation project, the contact was assumed to be stationary and a heat source was applied at the surface. This made it possible to only focusing on one of the contacts. When implementing movement in the master's thesis, it becomes necessary to have both a moving and a fixed contact in the same simulation. For that reason, the contacts should be heated up separately but cooled down together.

Implementing a reduced arcing time (i.e. change the arcing time to 2-4 ms)

The start of the arcing is different for making and breaking operation. During breaking, the arc ignites during the molten bridge phase as the high current density and short distance causes an electrical breakdown between the electrodes. This resulted in the ignition time to be equal to the opening time (i.e. t=0).

For the making operation, the igniting of the arc does not start at the same time as the contact starts to move. The ignition happens when the distance between the contacts are too short (i.e. the breakdown strength is lower than the present electrical field), causing an electrical breakdown to occur. Thereby, there are two variables causing ignition, the applied voltage and the distance between the contacts. Resulting in an ignition time not equal to the opening time (i.e. $t_{ignite} \neq t_{opening}$). In this master's thesis, it is assumed that the arcing time for the simulations is between 2 to 4 ms (i.e. starts 8 to 6 ms after closing has been initiating). This change is possible to perform by implementing a step function and a phase shift to the arc current.

Chapter 3

Theory and Literature Review

Electrical switching devices are complex. They need to be secure from both mechanical and electrical stresses and always react to the given command. To prevent unwanted stresses, they should be able to conduct any currents when in the closed position and be an excellent insulator in open position. Additionally, they should be able to transit smoothly to avoid the making and breaking of the current to decrease the capability of the switching device.

During closing operation, the switching device is subjected to its rated voltage until a breakdown occurs between the contact. The breakdown causes a short-circuit current to flow between the contacts, creating an electrical contact. This short-circuit current is called a *pre-strike arc* and occurs before the there is any mechanical contact between the electrodes. Consequently, the switch is in an electrically conductive state without mechanical contact. This pre-strike arc affects the capabilities of the switchgear causing melting, erosion, deformation and decreased mechanical and electrical properties. The amount of energy dissipated from the pre-strike can be calculated by Equation (3.1) [1], [9].

$$E_{Dissipated} = \int_{t_0}^{t_{end}} I_{sc}(t) \cdot V_{arc}(t) \, dt \tag{3.1}$$

$E_{Dissipated}$	Dissipated energy generated from the arc [J].
I_{sc}	Short-circuit current flowing between the contacts after a breakdown has occurred [A].
U_{arc}	Arc voltage [V].
t_0	Time of breakdown and ignition of the pre-strike arc [ms].
t_{end}	Time of mechanical touch and quenching of the electrical arc [ms].

17

This chapter first explains the important factors of the switching device. Factors such as the requirements, stresses and making and breaking capabilities of the switching device. This is followed by the breakdown mechanism during closing operation, where the breakdown in both gas-filled and vacuum are explained. Last, the phenomenon arc welding is explained, where the effect and consequences are described.

3.1 Requirements of Switching Devices

Switching devices has four requirements they must fulfil to be fully functional. These four requirements are:

i.   *Electrical conductor when in the closed position.*

In the closed position, the electrical conductivity in the contact must be extremely high to prevent generating of heat and a temperature increase. Heat is generated by ohmic losses present at the contact surface. To prevent heat generation and increased temperature, there must be a low resistance present. The only way to obtain a high rated load is when the contact resistance is low. The switch should be able to conduct all types of current, from short circuit current (for maximum 1-3 seconds) to continuous load current for long time [1], [9].

ii.   *Must be able to interrupt any currents when it in the closed position, without generating unacceptably large overvoltage.*

Switching devices should be able to interrupt all kinds of current at any given time. The requirements depend on the type of switching device. For instance, circuit breakers should be able to interrupt short circuit current present. While load break switches should be able to interrupt the nominal rated load current present. This requirement is important as the consequences of not responding to the faults can cause damage to power components present in the electrical network. Figure 6 illustrates the mechanisms occurring during opening of the contact [1], [9].
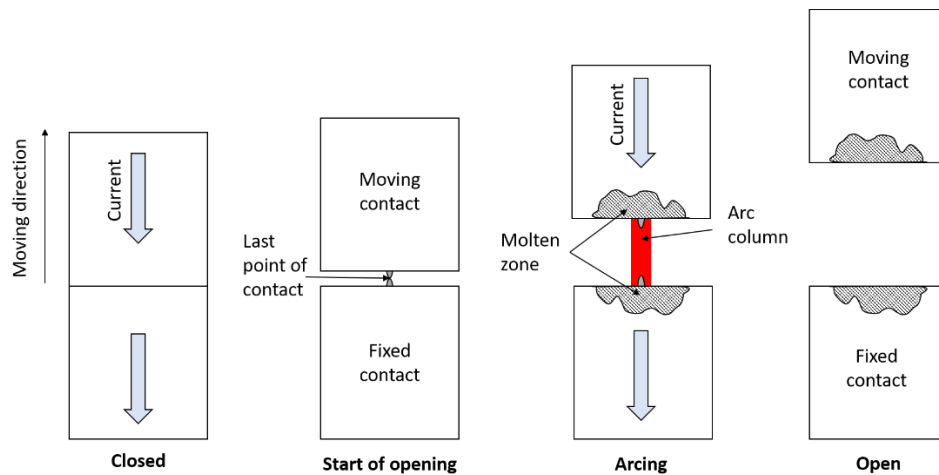
Figure 6: An illustration of the mechanisms occurring during breaking operation of an electrical contact. As the contacts starts to separate the contact points decreases down to a few. The decrease in contact points increases the current density, resulting in the contact point to melt and an arc to ignite between the contacts. The arc burns until it quenches resulting in a melted contact surface and some of the contact mass may have been eroded away.

iii.   *Excellent insulator when in the open position*

In the open position, the electrical conductivity must be equal or almost zero to become an excellent insulator. It should withstand all possible stresses (mechanical-, thermal- and dielectric stresses) during the entire breaking operation. Additionally, the switching device must remain open regardless of what is happening elsewhere in the electrical system. This includes power frequency overvoltage, rated voltage and transient overvoltage (i.e. lighting strikes and switching operations). A critical parameter for successfully becoming an insulator is the dielectric strength in the airgap. The dielectric strength needs to build up fast right after arc quenching to prevent re-ignition of the arc [1], [9].

iv.   *Must be able to close the contact at any time*

Switching devices should be able to close the contact when in the open state, although there is a short-circuit present. They must withstand numerous opening and closing operations throughout their lifetime. If the switching device is frequently opened and closed, it is important that the contact erosion remains low. Additionally, the switching device must be constructed to prevent the electrodes from welding together when closing. The maximum required making current depends on the power components presents in the electrical network. The device must be chosen with regards to the maximum stress present in the electrical system. Figure 7 illustrates the closing mechanism of a contact [1], [9].
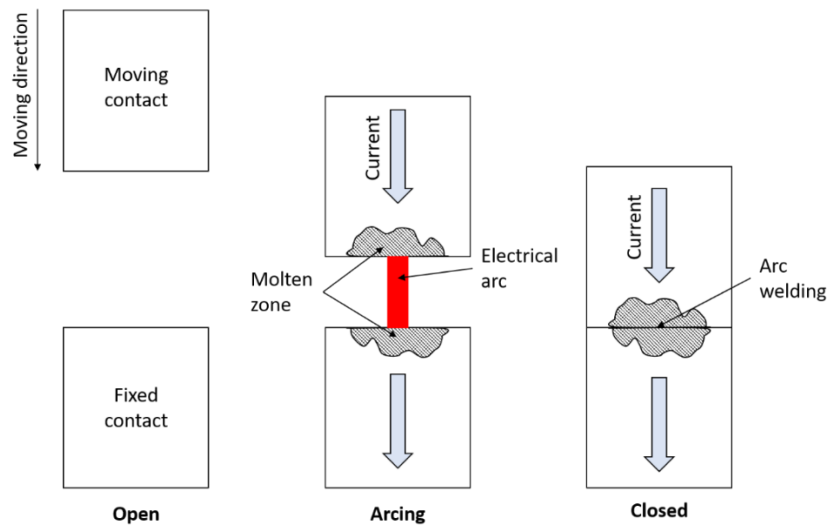
Figure 7: An illustration of the mechanisms occurring during making operation of an electrical contact. The moving contact moves towards the fixed contact. When the electric field between the contact overcomes the breakdown strength of the insulation medium, an arc ignites. The arc burns until the contact mechanically touches. At this point the molten metal generated during arcing fuses together and creates an arc weld between the contacts.

3.2 Stresses on Switching Equipment

Switching devices are exposed for various stresses when in operation. These stresses depend on the position of the switching contacts, i.e. open, closed or in the transition stage (opening or closing). There are three main stresses that must be taken into consideration when designing a switching device. These are mechanical-, dialectical- and thermal stresses. The outcome of the stresses can influence the contact materials, operation mechanism and the size of the switching device.

3.2.1 Mechanical Stresses

Several types of mechanical stresses are present during operation. The first mechanical stress normally mentioned is the switching stresses. Modern switching devices are moving very fast during interruption. The fast acceleration and deacceleration causes high stresses to both the mechanical system and the moving contacts. The stresses are highest at the start and end of a switching operation, i.e. when the acceleration is highest. The switching device should be able to open and close several thousand times when there is no current present (only mechanical forces) [1], [9].

Another mechanical stress present during switching, is the pressure increase during interruption. During interrupting, the energy dissipated is converted to heat, causing the pressure to increase inside the arcing chamber. If oil is used as the insulation medium, pressure can become a substantial problem. During interruption, the arc evaporates oil causing a substantial pressure increase inside the arcing chamber. When gas is used as the insulation medium, the effect of pressure is lower. This is a result of gas being compressible and oil being incompressible. The stresses caused by pressure increases with increasing current. Therefore, the size and wall-thickness of the pressure chamber is designed depending on the current level and dissipated energy.

The last of the mechanical stresses is generated by the Lorentz force (electromagnetic force). Lorentz force is generated from an electric field present around the contacts. The force is given as the vector product between the current density $\boldsymbol{J}$ and the magnetic flux density $\boldsymbol{B}$, as presented in Equation (3.2).

$$F_{Lorentz} = \boldsymbol{J} \times \boldsymbol{B} \tag{3.2}$$

Flux density $\boldsymbol{B}$ is directly proportional to the current. This make the force between the two electrodes proportional to the squared value of the current. When increasing the distance between the conductors, the force decreases due to the reduced magnetic flux density [1].

From these stresses, switching devices must be designed to withstand continuous mechanical stresses present in closed or open position and the rapid mechanical stresses occurring during the transition stage.

3.2.2 Dielectric Stresses

The dielectric stress is a result of interrupting an arc. Switching devices is required to be a perfect insulator in the open position, resulting in high requirements for the insulation medium. The insulation medium serves as the conductive-, interruption- and insulation medium and it is an important factor inside the switching device. It should maintain a high dielectric strength right after interruption and obtain a rapid recover of the dielectric strength [1].

Generally, the interruption of the arc occurs before the contact is fully open. This causes the insulation medium to have reduced dielectric strength compared to a fully open contact. The consequences of reduced dielectric strength right after interruption is re-strikes. If the arc re-

ignites after being interrupted, there is a longer arcing period and an increased thermal stress towards the electrodes.

The dielectric stresses are more critical during breaking operation due to the reduced dielectric strength right after interruption. The concerns of obtaining a re-strike between the contacts makes it necessary to choose a good insulation medium that fulfils the requirements for the switching device.

3.2.3 Thermal Stresses

The thermal stresses is produced by an increased temperature inside the switching device. The heat generated is caused by two different types of currents. These are:

i.   Short-circuit current present during faults.
ii.   Continuous rated current present during normal drift.

The difference is the magnitude and time period the current is present. The short-circuit current has a higher magnitude but is only present for a few milliseconds. During making and breaking operation an arc is ignited between the contacts. The energy dissipated from the arc is converted into heat melting the contact surface. This current causes a short-term heating on the contacts and other vital parts inside the switching device [1], [9].

Even though the magnitude of the short-circuit current is much higher compared to the continuous rated current, the thermal stresses is highest during normal operation. The thermal stresses are formally caused by the electric resistance in the joints, contacts and termination during normal operation. In closed position, the low contact resistance causes a low generation of heat. With time, this creates a high thermal stress. The most exposed places are those with low electrical conductivity, e.g. the boundary between the contacts, in sharp corners and at terminations. One of the main contributions to heating is a rough surface between the contacts. Rough surfaces results in few contact points and higher contact resistance [1], [9].

Cooling is a measure used to reduce the thermal stresses. By removing the generated heat as fast as possible, a lot of the thermal effects are neglected. Without an accumulation of generated heat, it is not possible to achieve an unacceptable high temperature resulting in

melting and evaporation. In addition, during arcing the cooling must be sufficient to reduce the temperature to prevent a thermal re-ignition.

The effect of thermal stresses can be [1], [9]:

- Erosion and deformation of the electrical contacts.
- Lowering the electrical conductivity (i.e. increase the electrical resistance).
- Increased pressure inside the arcing chamber.

3.3 Making and Breaking Capacity of Switching Devices

In addition to current interruption, connecting and disconnecting various power network components is one of the most important functions of switchgears. Making and breaking capacity denotes the maximum current a breaker can make or break during opening or closing of an electrical switch.

Breaking capacity is the maximum current, in rms, a switching device can interrupt during opening operation. Short-circuit currents exceeding the capacity, prevents interruption and quenching of the arc. The effects of not interrupt the arc can cause high thermal stresses on the contacts. The capacity is proportional to the gap distance and interruption medium. Increasing the gap distance or changing the interruption medium, e.g. air with SF_6, is the two main methods to increase the breaking capacity [1], [9].

Making capacity is the maximum current, in peak value, a breaker can conduct during closing operation. It is the value of the first cycle when there is an imaginary short-circuit between the phases (i.e. prospective short-circuit current).

As they are defined as rms- and a peak-value respectively, the making capacity are usually higher that the breaking capacity. Additionally, the DC offset is included in the making capacity not in the breaking capacity as it expires rapidly during breaking operation. This implies that the pre-strike arc present during making operation is more demanding to quench compared to the current present during breaking operation

Switching devices should be able to break and make the breakers full short-circuit current several times before replacement. The device must be designed to break the normal load current a few hundred to thousand times before being replaced [9].

3.4 Breakdown Mechanisms During Closing

Breakdown occurs when the insulating capabilities of a gap failures, causing a current to flow. This effect is usually caused by high electric field over the insulation. An electrical breakdown can be momentary during an electrostatic discharge or continuous as a burning electrical arc. A breakdown is necessary for an arc to initiate as the insulation medium need to lose its insulation capabilities and become conductive. The breakdown mechanisms act differently, depending on the presence of an insulation gas or not. Hence, this section explains both breakdown mechanism in gas-filled and vacuum switching devices.

In encapsulated systems the gas pressure has a major role in the breakdown strength of the insulation medium. Paschen curve presents the relationship between the gap distance, pressure and breakdown strength of encapsulated systems. Figure 8 presents the Paschen curve for air.
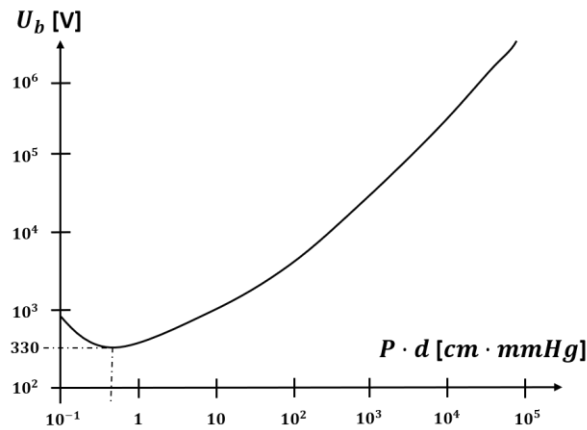
Figure 8: The curve presents Paschen curve for air. U_b is the breakdown voltage and $P \cdot d$ is the pressure multiplied by the distance between the electrodes [10].

An increased pressure inside the encapsulated system increases the gas density. Consequently, the distance between the gaseous particles decreases resulting in the electrons to not accumulate enough kinetic energy before colliding. To produce an ionization collision, the applied electric field can be increased to overcome the short distance between the particles. Thus, increasing the breakdown strength over the gap, as presented in Figure 8. Decreasing

24

pressure yields a decreased gas density. Hence, electrons require lower applied electrical field to produce an ionization collision. If the pressure decreases until vacuum is obtained, the breakdown strength increases as there are no particles present in the contact gap, resulting in no ionizing collision [10].

3.4.1 Breakdown in Gasses

SF_6 is commonly used as electrical insulation in switching devices due to its high breakdown strength, high recovery rate and its high electronegativity causing it to quench arcs faster. One disadvantage, SF_6 is a greenhouse gas that is more than 20.000 times higher than CO_2 and a leakage is highly damaging towards the environment. Air is another commonly used insulation gas. Air has lower breakdown strength than SF_6, but does not cause environmental problems. Due to its low breakdown strength, switching devices using air is bigger than switching devices using SF_6. Air is a self-recovering gas after breakdown, a cheap alternative to SF_6 and it is easy to inspect and maintain [10].

3.4.1.1   Ionization Processes for Gasses

The increased number of electrons and ions is the main reason of an electrical breakdown between the contacts. The generation of these particles are caused by ionization. There are three ionization mechanisms:

- Radiation (photo ionization).
- High temperature (thermal ionization).
- Electron impact (elastic and in-elastic collision).

Where electron impact is by far the most important mechanism present during ionization in gas filled switching devices.

Photo Ionization

Ionization caused by radiation is called photo ionization. A gas particle, i.e. atoms and molecules, can be subjected by radiation causing the particles to absorb photons. If the energy in the photon is sufficient, a single collision between a gas particle and the photon may cause

releasing of an electron resulting in generation of a positive ion. An illustration of photo ionization has been presented in Figure 9 [10].
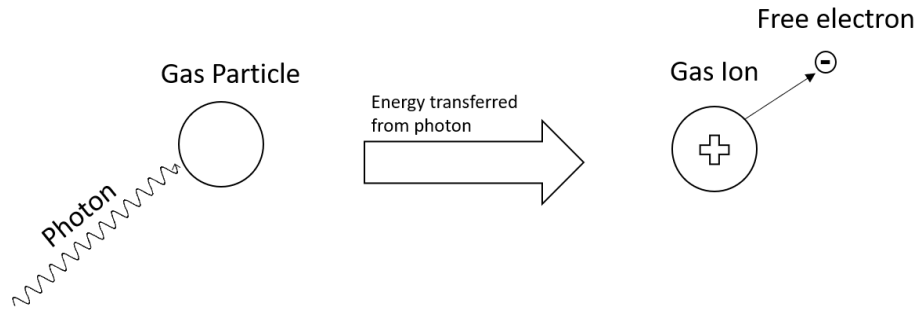
Figure 9: Illustration of photo ionization. The photon collides with a gas particle, transferring energy causing an electron to be released.

Thermal ionization

All gas particles have a mean kinetic energy directly proportional with the increase and decrease in temperature. When the temperature increases the gas particle may exceed the energy required for ionization. This may result in generation of new ions and electrons. If the temperature does not exceed the ionization energy, the energy from an electron collision or radiation can cause ionization. In this case, the energy needed from the photons or collision is lower compared to an insulation gas at room temperature. This makes it possible to get an ionization with longer wavelength or at lower movement speed. This implies that the breakdown strength is heavily dependent on the temperature. Figure 10 presents the process where a gas molecule is ionized due to increase in temperature [10].

Figure 10: Illustration of thermal ionization. If a gas particle is exposed for heat such that the internal temperature increases, the gas particle can get excited and cause an electron to be released.

Ionization by collision

During breakdown in gasses, collision ionization is the most important mechanism for ionization. During collision the amount of energy transported between the particles depends on if there is an elastic or an inelastic collision [10].

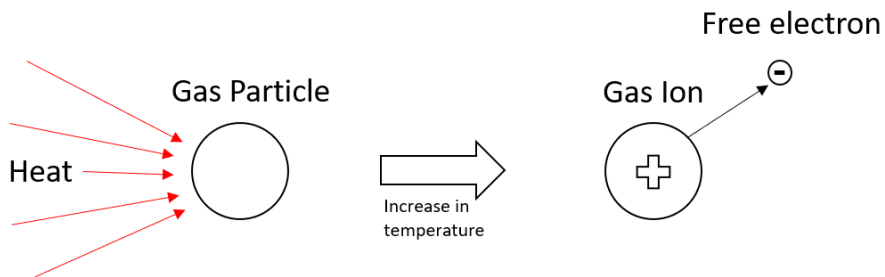**For elastic collision,** the total kinetic energy is preserved during the collision. That means that all the moving energy is converted from one particle to another. An elastic collision will not cause ionization of the insulation gas. Therefore, it is only necessary to examine the inelastic collision to find the ionization mechanism.

For inelastic collision, the total kinetic energy is not preserved during collision. Here, some of the energy before collision is converted to another state of energy. Normally this new state of energy is heat or most important ionization energy. The energy released during collision is the most important factor contributing towards ionization. The higher the velocity, the higher the probability for ionization. Hence, for an ionization caused by collision, these factors are essential:

- **An inelastic collision:** The collision between particles and the insulation gas must be an inelastic collision. The energy transformed into ionization energy is only present in an inelastic collision.
- **A charged particle:** The moving particle must be either an electron or an ion. The highest chance for ionisation is with an electron, but there is still a possibility for ionization with an ion.
- **High velocity:** The moving particle should travel with a high velocity. A high velocity of the particle increases the probability for ionization.

3.4.1.2 Breakdown Mechanism in Gasses - Streamer Mechanism

A big group of electrons and ions is called an *electron avalanche*. Avalanche is assumed to move towards the anode with the speed of the electrons. The big difference in mass between ions and electrons inside the avalanche causes the electron to move with a higher velocity. It can therefore be assumed that the ions are stationary compared to the electrons. Thus, the length

of the avalanche increases with the movement of the electrons. This has been illustrated in Figure 11.

The shape of an avalanche is given by the size difference between an electron and an ion. The variation in inertia, due to the large mass difference, gives the avalanche a droplet shape. Electrons move towards the anode with a higher velocity compared to the ions movement towards the cathode. This can be described as ions *"lags behind"* the movement of the electrons. Figure 11 illustrates the shape of an avalanche [10].
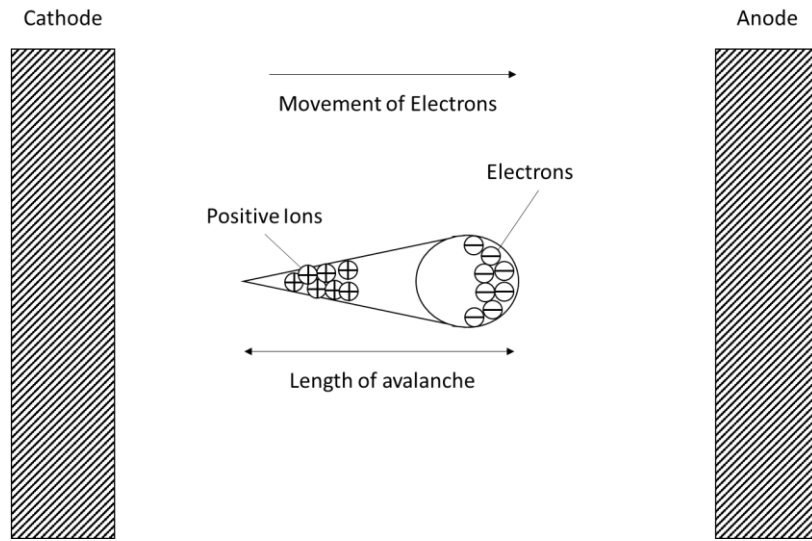
Figure 11: An illustration of the droplet shape of an electron avalanche. The electrons are moving towards the anode with a higher speed than the positive ions travel towards the cathode. This causes the avalanche to have a droplet shape.

Theoretically, a breakdown can be the caused from a single avalanche, but the probability is higher for each avalanche present. A single avalanche can be the cause of breakdown due to the energy stored in the ionic gas (i.e. electrons and ions). The energy can be emitted as photons and cause photo ionization and forming of new avalanches. The new avalanches can emit photons and cause new ionizations, causing new avalanches resulting in an increased number of electrons as illustrated in Figure 12.
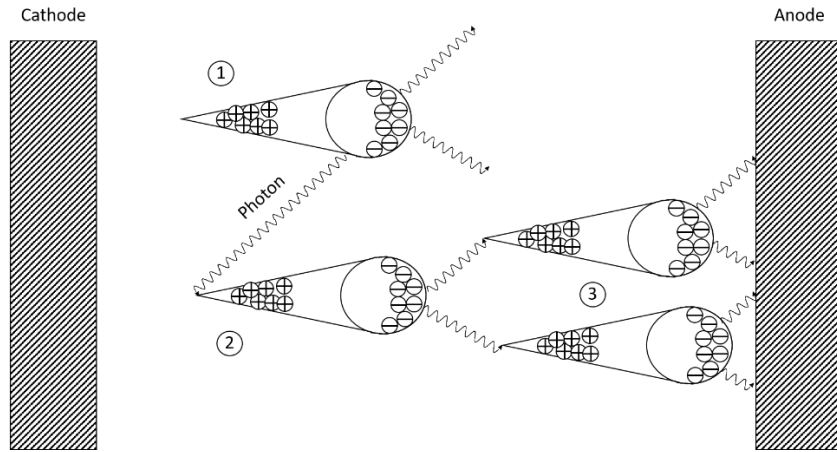
Figure 12: An illustration of streamer mechanism before the first avalanche hits the anode. (1) The first produced avalanche emits photons that causes a new avalanche to be formed. (2) The new avalanche is similar to the first avalanche, emitting photons that can causes two new avalanches. (3) The probability for generating new avalanches are higher for each generated avalanche.

The generated avalanches will eventually collide with the anode, causing a locally enhanced electric field. Comparing the inertia of the ions and electrons, it can be assumed that ions stands still, forming free space charges around the anode. These space charges cause an extension of the anode. The moving avalanches are drawn towards the higher electric field. A long line of avalanches is formed, called a streamer. The streamer builds up as a long chain and will eventually reach the cathode, making a free conductive path between the cathode and the anode. This results in a breakdown and ignition of the electrical arc. The streamer mechanism is presented in Figure 13 [10], [11].
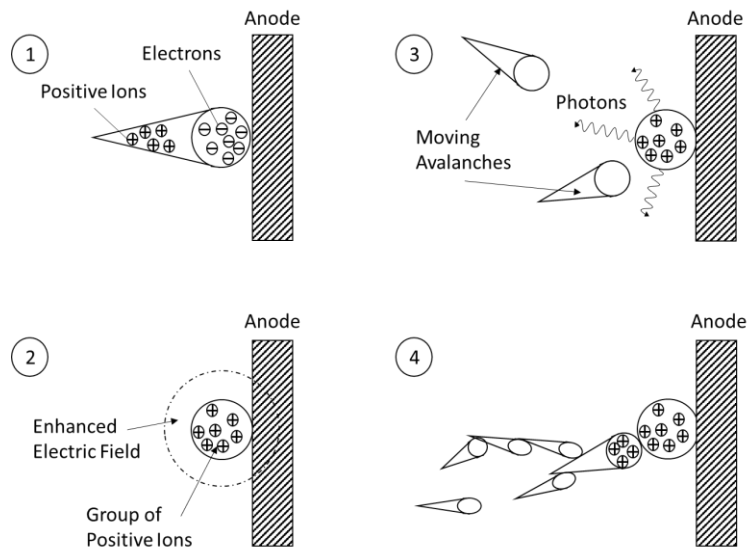
Figure 13: An illustration of the streamer mechanism. (1) An avalanche collides with the anode, (2) causing the ions to become free space charges. These space charges make a enhances electric field at the tip of the electrode. (3) The moving avalanches are drawn towards these space charges, collides and gets combined. (4) This long chain of avalanches eventually reach the cathode resulting in a breakdown between the electrodes.

3.4.2 Breakdown in Vacuum Breakers

In vacuum breakers, no insulation medium is present. Thus, ionization is not initiated by collision. Other mechanisms are therefore required for a breakdown to occur. In vacuum breakers, the main ionization mechanism is electron emission from the contact surface. The electrons emitted are due to the high electric field (field electrons) and the high temperature (thermal electrons). The electrons emitted due to the high electric field may produce a higher temperature locally due to the increase in contact resistance. The increased temperature results in more emission of temperature electrons [1], [12].

The increase in temperature may exceed the melting temperature causing a local melting of the contact material. If a significant amount of material has melted, the molten material might explode at the cathode. The explosion sends out a mixture of metallic vapour, electrons, ions and metallic atoms and molecules to the contact gap. This effect is called *explosive electron emission*. High temperature creates plasma around the contact surface due to the explosion, making it easier for the electrons to move towards the cathode. New particles floating around between the contacts can be ionized by the accelerating electrons moving towards the anode. Resulting in new generations of ions and electrons [1], [12].

The explosions at the cathode cause small holes to appear at the contact surface, called *cathode spots*. Figure 14 presents an illustration of cathode spots and the particles emitted from the contact surface. Each explosion has a cone-shaped structure, when sending out the free particles. Close to the contact surface at the cathode, a region full of positive space charges (positive ions) are formed. This is a result of the attraction between the negative charged cathode and the positive charged ions. When traveling further away from the cathode, a metallic vapour plasma is present. This metallic vapour plasma have a decreasing density with increased distance from the cathode [1], [12].
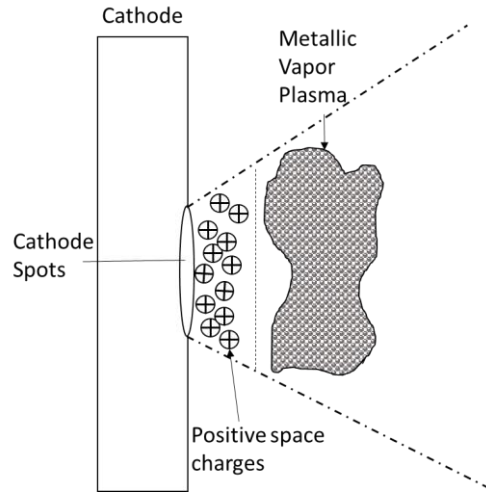
Figure 14: An illustration of the different particles present in the gap between the electrodes for a vacuum circuit breaker. Closest to the cathode spots is a layer of positive space charges. Traveling further away from the cathode spot is a metallic plasma. The plasma density decreases with increasing length away from the cathode spot.

The number of electron emission is highly dependent on the current level present and the contact material. It is important to mention that the vacuum breakers have different arcs depending on the current level. The two types of arc are *diffuse mode vacuum arc* and *constricted mode vacuum arc*.

For low currents (below 10 kA), the diffuse mode vacuum arc is active. In this type of arcs a lot of small cathode spots appears at the cathode. There is no well-defined arc column, only many small arcs between the contacts. The low amount of dissipated energy is not sufficient in order to create a wide area of conductive plasma. This type of arcs is characterised by low contact erosion and weak light emitting during arcing. In diffuse mode vacuum arcs, the anode is in the passive stage, where it only absorbs the colliding electrons. There is no visible footprints at the anode after arcing. The low amount of dissipated heat after current zero, result in a fast switching gap recovery. Hence, the current is easily made and interrupted. Figure 15 illustrates the structure of a diffuse mode vacuum arc [1], [12].
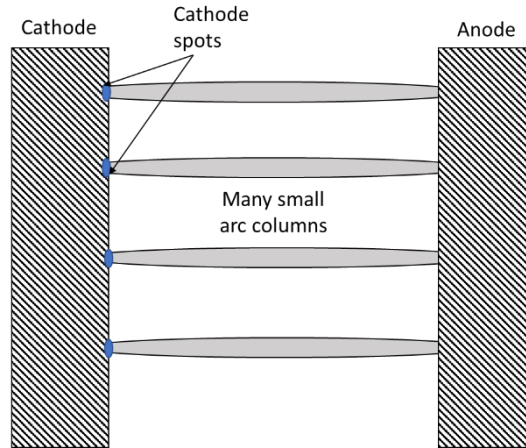
Figure 15: An illustration of the diffuse mode vacuum arc. In this case there is many small arcs forming between the electrodes. The low amount of dissipated energy causes the arc columns to not combine and form one big arc.

For higher currents (above 10-15 kA), the constricted mode vacuum arc is active. The behaviour of the arc changes significantly, depending on the geometry of the contact and the contact material. The high short-circuit current increases the amount of dissipated heat, causing the cathode spots to gather towards one point, making one well-defined arc column. Due to the increase in temperature, both the anode and cathode melts and contribute to the amount of metallic vapour in the contact gap. This results in formation of cathode- and anode spots. The characteristics of a constricted mode vacuum arc is similar to a high-pressure arc (i.e. gas filled circuit breakers). There is a distinctive anode and cathode spot after arc extinguishing, resulting in high contact erosion. Additionally, the arc is harder to interrupt, due to the increased amount of free metallic vapour in the switching gap. Therefore, entering into constrictive mode arcs is clearly undesirable, and should be avoided during the operation of vacuum switching components. Figure 16 illustrates the structure of a constricted mode vacuum arc [1], [12].
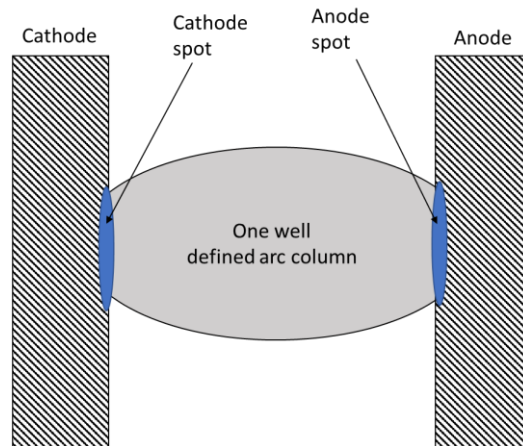

Figure 16: An illustration of the constricted mode arc. In this case all the cathode spots forms into one wide area of molten material. The results in one well-defined arc column.

32

When the current exceeds its peak value, the amount of dissipated energy decreases. The cooling will at some point overcome the generation of heat resulting in a decreasing temperature. This causes the cathode spots to extinguish one by one, reducing the amounts of burning arcs. Normally, the arc quenches at the natural current zero crossing, but in some cases the arc can quench before this value. This is called *current chopping* and typically occurs in vacuum breakers. Current chopping is always unwanted due to the rapid change in current, which can lead to overvoltage in the system. Therefore, it is important to choose a contact material producing a low chopping current [1], [12].

In summary, breakdown in vacuum circuit breakers are mostly dependent on the amount of emitted material from the electrodes. Thus, the contact material is an important factor towards a good and stable arc. Vacuum circuit breakers are mostly desirable to use at low currents. Additionally, the amount of eroded material for each operation must be taken into consideration, especially when a vacuum circuit breaker opens and closes frequently.

3.5 Arc Welding – Concerns When Closing an Electrical Switching Device

A major part of this master thesis is to examine the effects a pre-strike arc has on the contact materials during making operation. As explained earlier, the electrical arc can cause melting, erosion and deformation of the contacts. Additionally, the mechanical and electrical properties can become weaker.

A concerning problem with closing a contact is the risk of arc welding. Once the pre-strike arc is formed between the electrodes, it causes melting of the contact material. During mechanical touch between the two electrodes, the liquified material fuses together creating a mechanical contact. At this point, the pre-strike arc quenches and no heat source is currently present, except from the contact resistance. This causes the temperature at the contact to decrease and the liquid metal to solidify, creating a weld between the electrodes. The newly created weld may prevent the switchgear to properly response to the next opening command. This occurs when the force generated from the switching operation is insufficient to break all the welding points [1], [9].

Serious problems can occur if the strength of the weld overcomes the forces generated from the mechanical movement. The force needed to break the weld depends on the contact material and the area of the welding. Equation (3.3) presents the welding force of the contacts [9].

$$F_w = \Gamma \cdot A_w \qquad (3.3)$$

F_w Force needed to break the weld [N].

Γ Ultimate tensile strength of the contact material that has been welded [Pa].

A_w Total area of the contact weld [m^2].

Figure 17 illustrates the area of the weld. In this master's thesis it is assumed that the arc weld is circular to simplify the calculation of the arc weld area [9].
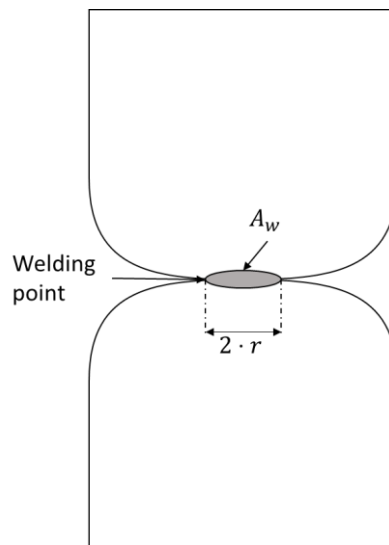
Figure 17: An illustration of the arc welding area when two electrodes are welded together. It is assumed that the weld is circular [9].

Chapter 4

Methodology - Modelling of the System Using COMSOL Multiphysics®

In this master's thesis, COMSOL Multiphysics is used to simulate the temperature distribution, erosion rate and arc weld strength of a medium voltage switching device. The physics used are *Heat transfer in liquids* and *Deformed Geometry*. Heat transfer in liquids determines the temperature distribution in an object exposed for heat flux. The simulated object can be in solid and liquid state simultaneously, making it possible to include a phase change. The phase change updates the material properties when exceeding the melting temperature. Deformed geometry is used to determine the erosion rate of the model. The geometry deforms when the temperature increases above the evaporation temperature. Additionally, it is possible to include the movement of the contact during closing operation [13].

The model is studied in a time dependent domain, as temperature requires time to build up and distribute throughout the geometry. For simplicity, the pre-strike arc was substituted by a heat source and applied at the boundary of the contacts, resulting in a simulation with reduced complexity. An electrical contact is a symmetrical object, thus 2D axisymmetric has been used to model the geometry.

This chapter explains in detail the different parts and boundary conditions that has been included in this simulation model.

4.1 Problems Occurring During Modelling

During the modelling process two problems occurred, causing the model to not fully operate as intended. These were the modelling of the material distribution (cubical shape) and the movement of the contact (temperature distribution).

4.1.1 Cubical Material Distribution

It has previously been described that the contact material consists of individual copper and tungsten particles that are sintered together. The outcome is a contact material that has one continuous copper layer with tungsten particles trapped in between. Therefore, a cubical material distribution was tested, in order to make the material distribution more realistic. In this case each cube were either copper or tungsten, as illustrated in Figure 18.

The problem occurred when the contact surface started to move and erode. When simulating, the geometry responded incorrectly towards the movement and erosion commands, causing the simulation to crash after a short time period. One explanation for this problem could be the increase in boundaries inside the model. Most likely, the boundaries started to conflict with each other, resulting in a model with little freedom.
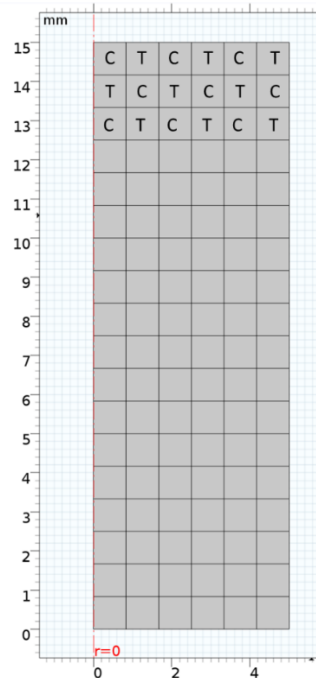
Figure 18: An illustration of the cubical model that was tried when simulating copper-tungsten as the contact material. The "C" areas correspond to copper, and "T" to tungsten. The contact material continues with the same pattern as shown.

4.1.2 Movement of the Contact Influencing the Temperature Distribution

The next problem occurred when simulating the movement of the contact. It was observed that the movement of the contact influenced the temperature distribution inside the object. Movement of the contact is implemented by adding a mesh velocity to the boundaries placed perpendicular to the moving direction. The mesh velocity causes the model to be stretched at the boundary subjected for heat source and compressed at the opposite boundary. This movement method is further explained in Section 4.7 *"Movement of the Contact"*.

The problem occurred during the stretching and compression of the contact surface. COMSOL assume that the temperature distribution inside the contacts are constant when mesh velocity stretches the contact. This implies that the stretched material has the same temperature as the boundary of the heated surface, which would not be the case in the real world. The resulting simulations showed a moving contact significantly hotter than the boundary of the fixed contact, as presented in Figure 19.

This was resolved by reducing the gap distance between the contacts. The contacts should be heated up separately but cooled down together. Implying that the contacts only influence each other at the point of mechanical touch. The gap was first set to be equal to 15 mm, but was reduced down to 0.15 mm after the problem was detected. With a gap distance of 0.15 mm, the temperature distribution during movement had a minor influence on the simulations.
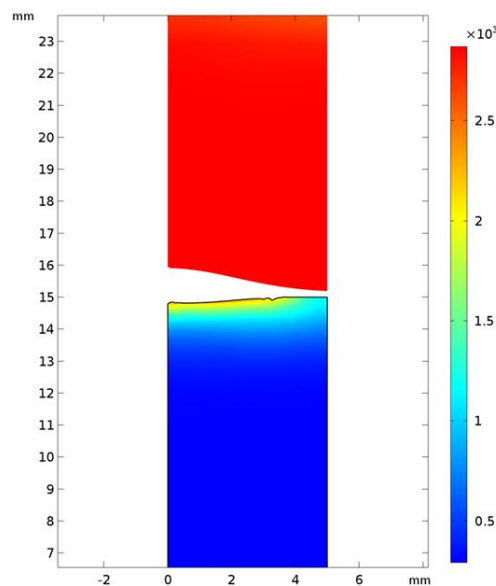
Figure 19: An illustration of the contact when the movement influenced the temperature distribution wrongly inside the contact material.

4.2 Geomatical Dimensions of the Model

The model consists of a fixed and a movable contact drawn as a 2D- axisymmetric model. During simulation, COMSOL revolves the model around the predefined axis, creating a cylinder. The geometrical dimensions have been set equal for both the anode and the cathode. The geometry was held constant for every simulation in order to compare the results between each type of simulation. The height and diameter were determined to be 15 mm and 10 mm respectively, resulting in a total volume of 1178 mm^3.

During simulation of the composite material, the geometry was divided into 4 layers. The first and third section were set to be copper and the remaining layers were tungsten. The thickness of each layer were 1.25 mm. Figure 20 and Figure 21 presents the three different contact materials examined in this master's thesis.

Table 2: Geometrical dimensions of the model used during simulations. The non-layered model is used when the contact consist of pure copper or tungsten. The layered model is used when simulating the composite material copper-tungsten.

Geomatical dimensions of the model		
	Width	**Height**
Non-Layered model	5 mm	15 mm
Layered model (of each layer)	1.25 mm	15 mm
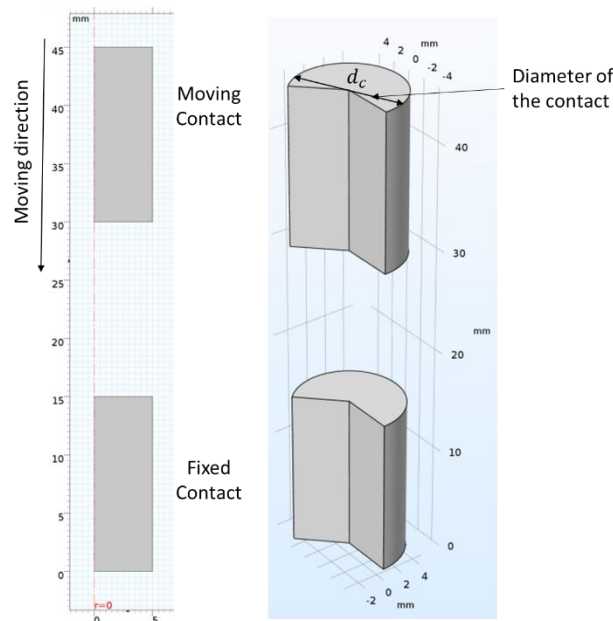
Figure 20: The geometrical shape of the non-layered model. In this case the model is purely copper or tungsten. In this figure the gap distance is 15 mm in order to give a better visual presentation, but during simulation the gap distance was 0.15 mm.
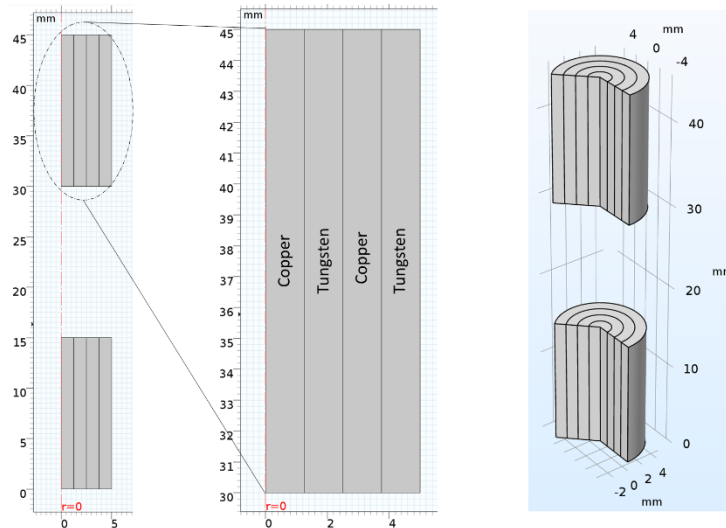
Figure 21: The geometrical shape of the layered model. In this case the model consists of 4 layers, where layer 1 and 3 is copper and layer 2 and 4 is tungsten. In this figure the gap distance is 15 mm in order to give a better visual presentation, but during simulation the gap distance was 0.15 mm.

4.3 Finite Element Mesh Selection

Meshing is a method where the geometry is divided into small elements. Each element has their own nodes. In-between the nodes, COMSOL Multiphysics® uses nodal approximation to calculate the values. Meshing simplifies the calculations and makes it possible to simulate highly detailed models with high precision. A high density of nodes increases the accuracy of the simulations. This implies that important parts of the model should have a high density of nodes.

There are two possible ways to divide the geometry into smaller elements, namely *Free Triangular* and *Free Quad.* The difference is the geometrical shape the nodes creates when using nodal approximation. As the name implies, the free triangular creates triangular shaped elements and free quad creates quadrilateral shaped elements, with three and four nodes respectively. Free quad has a higher precision than free triangular, but it lowers the model's freedom to move [2], [13].

In this project the mesh is an essential part of the simulation, since both a mesh movement and physical deformation of the geometry is applied. Therefore, building a detailed and continuous mesh is necessary. In this thesis, the most vital area is at the boundary of the contact surface where the heat sources are applied. For this reason, free quads has been used on the entire domain, to ensure a high accuracy of the results.

The mesh distribution depends on the contact material examined. When the model consists of pure copper or tungsten, the density is highest near the centre of the arc column and decreases outwards, as presented in Figure 22. When the composite material copper-tungsten is simulated, the highest density is also close to the centre of the arc column, as well as at the boundary between the layers. This implies that the highest density of nodes has been applied in layer 1 and 2, as presented in Figure 23.
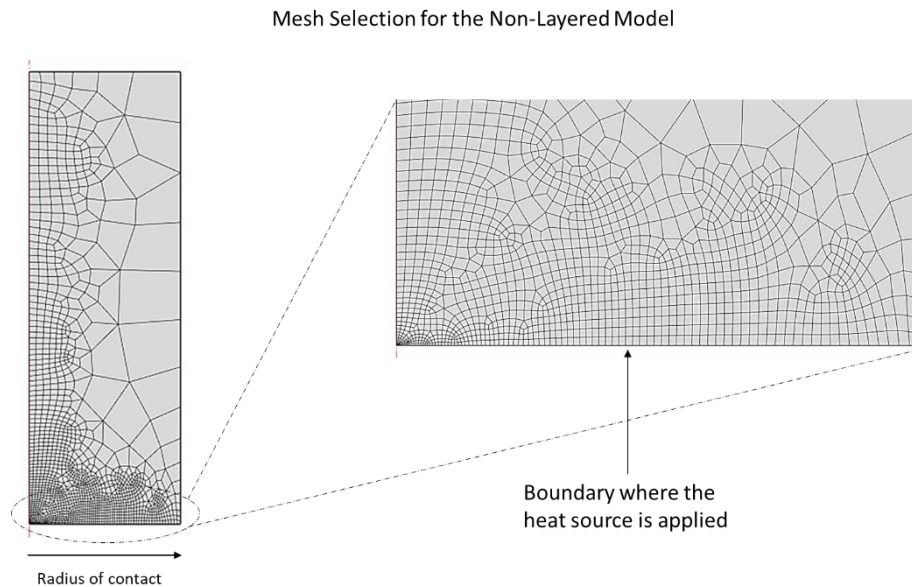
Figure 22: The mesh selected when simulating the non-layered model. In this case the highest density of nodes is close to the centre of the arc column (i.e. down in the left corner).
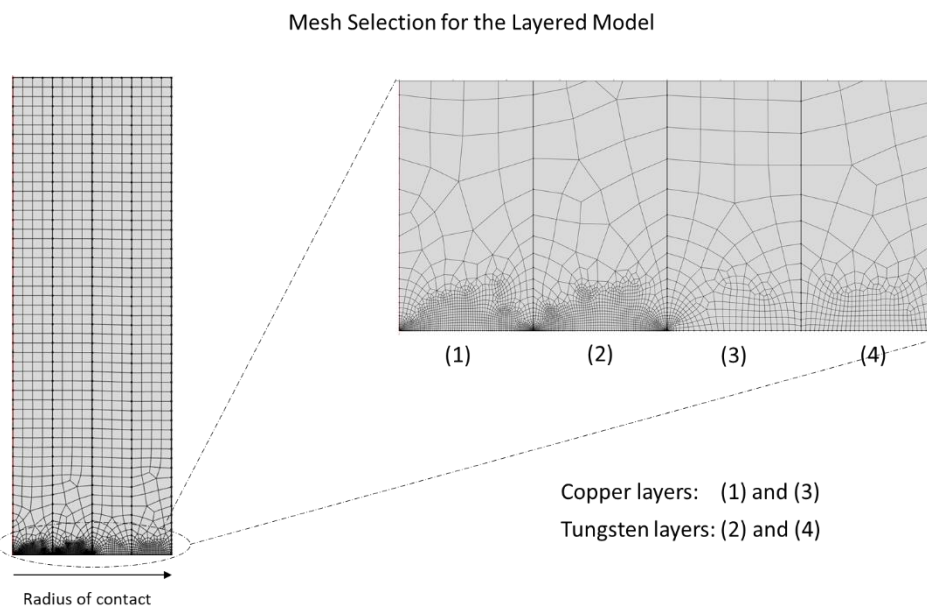
Figure 23: The mesh selected when simulating the layered model. In this case the highest density of nodes is closes to the boundary where the heat source is applied. Since layer 1 and 2 are closes to the arc centre, the highest density is in these layers.

4.4 Material Properties - Solid and Liquid State

Three different contact materials has been examined, copper, tungsten and copper-tungsten. During temperature simulation, some material properties has to be implemented. These are the material density, thermal conductivity and heat capacity of both copper and tungsten. Table 3 and

Table 4 presents the values of these properties in solid and liquid state respectively [2], [14]-[21].

Table 3: Material properties of copper and tungsten in solid state. The values are at ambient temperature (i.e. 20 ℃).

Material properties of in the solid state				
		Copper	Tungsten	Unit
Density	ρ	8960	19 300	$[kg/m^3]$
Thermal conductivity	k	400	175	$[W/m \cdot K]$
Heat capacity	C_p	385	132	$[J/kg \cdot K]$

Table 4: Material properties of copper and tungsten in liquid state. These values are assumed to be constant for the entire liquid phase [14]-[21].

Material properties of in the liquid state				
		Copper	Tungsten	Unit
Density	ρ	8020	17600	$[kg/m^3]$
Thermal conductivity	k	160	100	$[W/m \cdot K]$
Heat capacity	C_p	572	275.5	$[J/kg \cdot K]$

Heat transfer in liquids makes it possible to simulate a phase change, with use of the function *phase change material*. When exceeding the melting temperature, the material properties are updated. This function requires some new parameters, such as: melting temperature, latent heat of melting and the transition interval for the temperature. These values are presented in Table 5 [14]-[21].

Table 5: Material properties used when implementing the phase change from solid to liquid phase [14]-[21].

Material properties for phase change				
		Copper	**Tungsten**	**Unit**
Melting temperature	T_m	1358	4483	$[K]$
Latent heat of melting	L_m	207	192.5	$[kJ/kg]$
Transition interval for the temperature	ΔT	20	20	$[K]$

4.5 Heat Source Modelling – Pre-Strike Arc

To model an arc is extremely complex. The number of factors changing with time, temperature and conductivity causes an arc simulation to increase in complexity. Therefore, a simplification of the arc has been introduced into the model. The simplification is to swap the arc out with a heat source. The heat source is applied at the boundary of the material and has a value equal to the dissipated energy, as illustrated in Figure 24. Equation (4.1) presents the dissipated energy in the pre-strike arc.
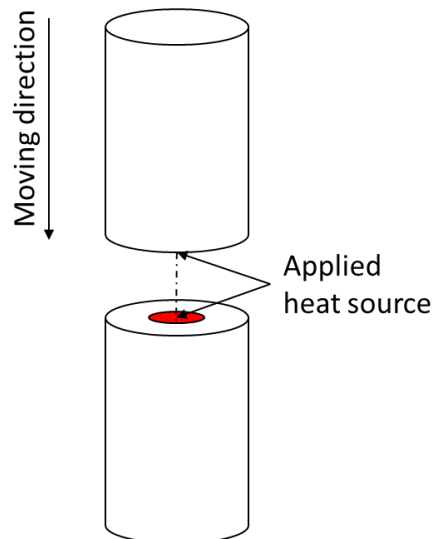
Figure 24: An illustration of the heat source applied at the contact surface of the contact. The centre of heat source is placed at the centre of the electrodes. The red zone indicates the applied heat source.

$$E_{Dissipated} = \int\limits_{t_0}^{t_{end}} I_{sc} \cdot U_{arc} \; dt \qquad (4.1)$$

$E_{Dissipated}$	Dissipated energy for the entire arcing period [W].
I_{sc}	Short-circuit current flowing between the contacts during the arcing period [A].
U_{arc}	Arc voltage [V].
t_0	Time when the arc ignites [ms].
t_{end}	Time when the mechanical contact touches and the pre-strike arc quenches [ms].

Fortunately, the pre-strike arc has a short time duration causing a low amount of dissipated heat and low contact melting. This duration is normally in the time range of 2-4 ms and is strongly depended on the insulation gas and the contact material. Figure 25 presents the gap voltage and arc current during a making process.

Before the ignition of the arc, the gap voltage follows the power frequency voltage. However, at arc ignition the gap voltage drops down resulting in the arc voltage. For all simulations the gap voltage is held constant for the entire arcing period. The making current through the airgap is zero before ignition, as there is no electrical contact. At breakdown the pre-strike arc ignites and causes a current to flow between the electrodes. At this point the current stars following with a sinusoidal shape, as illustrated in Figure 25.
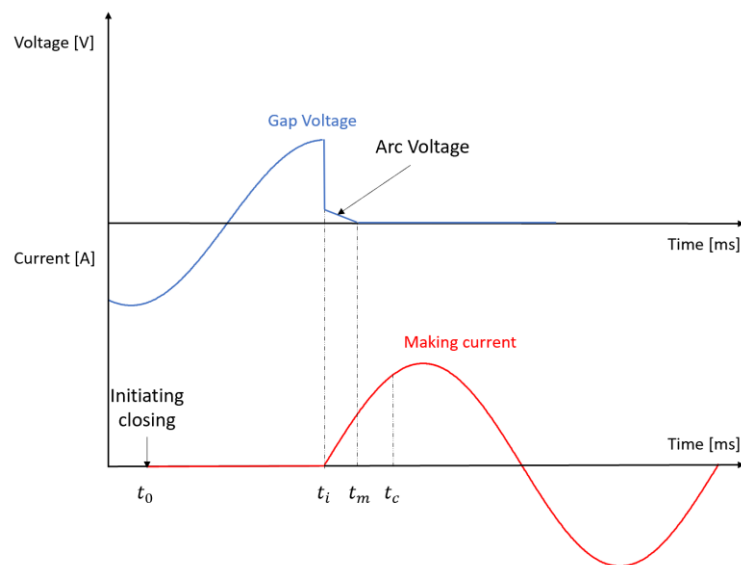
Figure 25: An illustration of the arc current and the gap voltage during a making process. The different time intervals are: t_0 initiation of closing, t_i the instant of pre-strike, t_m the instant where the contact mechanically touches and t_c the instant where the contact reaches the fully closed position. The arcing duration is the time between the time instants t_i and t_m.

To simulate heat generation from the pre-strike arc in COMSOL three modifications has been implemented. These are: a step-function, an angle displacement and an exponential function.

The step-function is implemented to make the heat source only active during the arcing period. The step-function changes between the values 0 and 1, meaning that during the arcing period the value is 1 and all other time instances the value should be 0. This is illustrated in Figure 26.
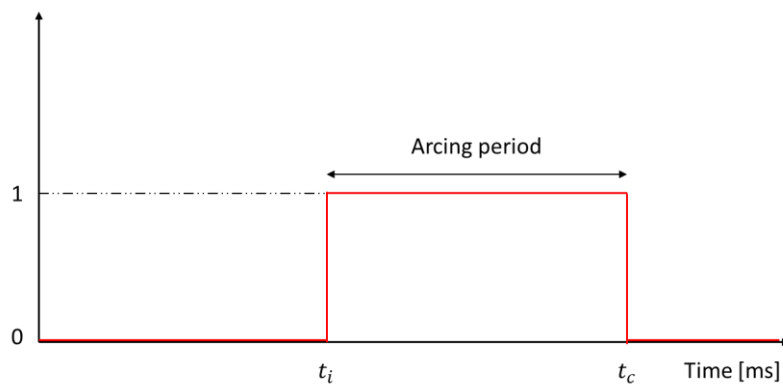
Figure 26: An illustration of the step-function implemented in the simulations. The value changes between 0 to 1 during the simulation interval. The time intervals are: t_i the instant of pre-strike and t_c the instant where there is mechanically contact.

The phase shift is introduced to the model, as the making current should start at zero, when the arc ignites. As previously mentioned, the arcing time is set to be 2-4 ms, implying that the pre-strike arc starts 6-8 ms after initiation of closing. The phase shift angle is calculated by using Equation (4.2) and Equation (4.3), were the time t_i is the instance when the arc ignites. Table 6 presents the values of the phase shift angle for different ignition times.

$$\sin(\phi + \omega t) = 0 \tag{4.2}$$

$$\phi = -\omega \cdot t_i \tag{4.3}$$

Table 6: Presents the different phase shift angles used during simulations.

Phase shift angle for different arcing times		
Time of ignition		Phase shift angle
t = 6 [ms]	ϕ	$-\dfrac{3}{5}\pi$
t = 7 [ms]	ϕ	$-\dfrac{7}{10}\pi$
t = 8 [ms]	ϕ	$-\dfrac{4}{5}\pi$

The last implementation is the exponential function. An electrical arc has a gaussian distribution where the temperature is highest at the centre of the arc column and decays outwards. To simulate this effect Equation (4.4) is implemented.

$$Exponential\ function = e^{-\left(\frac{l(r)}{r_{arc}}\right)^2} \tag{4.4}$$

$l(r)$ Distance from the centre of the arc column and outwards. This value changes with the radius r [mm].

r_{arc} Radius of the arc column [mm].

The final expression for the applied heat source at the anode and cathode is given in Equation (4.5) and Equation (4.6).

$$Q_{Anode} = Stepfunction(t) \cdot U_{Anode} \cdot \sqrt{2}\,I_{rms} \cdot \sin(\phi + \omega t) \cdot e^{-\left(\frac{l(r)}{r_{arc}}\right)^2} \tag{4.5}$$

$$Q_{Cathode} = Stepfunction(t) \cdot U_{Cathod} \cdot \sqrt{2}\,I_{rms} \cdot \sin(\phi + \omega t) \cdot e^{-\left(\frac{l(r)}{r_{arc}}\right)^2} \tag{4.6}$$

The voltage drop U_{Anode} and $U_{Cathode}$ is equal to 7.5 V and 17.5 V respectively. The voltage drop in the arc column is neglected, due to the short length between the contacts.

4.6 Vaporisation of the Contact Material

Vaporisation of the material is a key factor for finding the erosion rate on the contact material. During simulations, the model is exposed for heat flux causing the temperature to increase. With no boundary conditions, the temperature inside the model can increase without limitations. This provides a model that is unrealistic, and the test results becomes invalid.

To prevent this from happening, an upper limit of the temperature is implemented, inhibiting the temperature of the object to increase beyond this point. If the temperature in the contact material increases above this threshold, the material evaporates and disappear. In this thesis all evaporation is considered contact erosion. Evaporation causes a geometrical deformation and material loss when increasing above the vaporisation temperature.

The geometrical deformation is performed by using the physic deformed geometry. The used method deforms the geometry by applying an erosion rate at the boundary where the heat source is present. The equation for erosion velocity is expressed in Equation (4.7) [2], [22].

$$v_n = \frac{q_s}{\rho \cdot H_s} \tag{4.7}$$

v_n Material erosion velocity [m/s].

ρ Density of the material [kg/m^3].

H_s Heat of sublimation [kJ/kg].

q_s Ablative heat flux [kJ/m^2].

The ablative heat flux is the heat causing the surface of the contact to evaporate. This feature is implemented by using the function *Heat flux* under the physic heat transfer in liquids. The ablative heat flux is applied at the same boundaries as the heat source. COMSOL removes the contact material when the contact temperature (T_c) becomes higher than the vaporisation temperature (T_v). The ablative heat flux can be calculated by using Equation (4.8) [2], [22].

$$q_s = h_s \cdot (T_v - T_c)$$ (4.8)

T_v Vaporisation temperature [K].

T_c Contact temperature [K].

h_s Heat transfer coefficient changing with the contact temperature [1].

If $T_c < T_v$, h_s becomes zero, as there is no vaporisation present. If $T_c > T_v$, h_s increases linearly. The steepness of h_s is required to be large, preventing the contact temperature to markedly exceed the vaporisation temperature. Table 7 presents the different vaporisation temperatures for copper and tungsten [2], [22].

Table 7: Presents the vaporisation temperature for copper and tungsten.

Vaporisation temperature			
Material Type		**Temperature**	**Unit**
Copper	T_{vc}	2835	**[K]**
Tungsten	T_{vt}	5828	**[K]**

4.7 Movement of the Contact

The movement of the contact has to be introduced into the model when simulating the making process. As previously mentioned, the contacts should be heated up separately and cooled down together. The method used to implement a movement to the contact is by adding a mesh velocity to the boundaries perpendicular to the moving direction. The mesh velocity causes the model to be stretched at the boundary where the heat source is present and compressed at the opposite boundary. Equation (4.9) and (4.10) presents the equations applied at both boundaries. Figure 27 illustrates where the different normal mesh velocities are applied.

$$v_{n,compress} = Stepf(t) \cdot v_{contact} \qquad (4.9)$$

$$v_{n,\text{stretch}} = Stepf(t) \cdot v_{contact} + \frac{q_s}{\rho \cdot H_s} \qquad (4.10)$$

$v_{contact}$ — Velocity of the moving contact [m/s].

$v_{n,\text{stretch}}$ — Normal mesh velocity applied at the boundary where the heat source is applied [m/s].

$v_{n,compress}$ — Normal mesh velocity applied at the boundary opposite of where the heat source is applied [m/s].

$Stepf(t)$ — Step-function introduced to make the contact velocity start at initiation of closing and end at mechanical touch between the contacts [1].
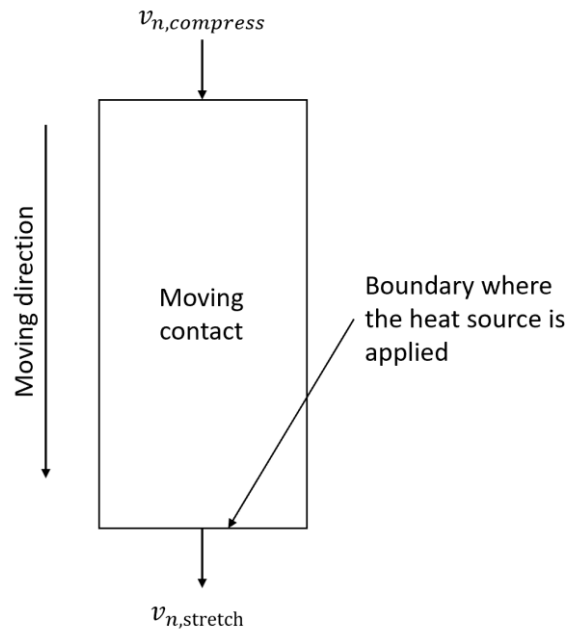
Figure 27: Illustration of the applied normal mesh velocity. The compressed velocity is applied behind the contact, causing it to "push" the contact boundary downwards. The stretching velocity is applied at the boundary, where the heat source is applied, causing it to "pull" the contact boundary downwards.

4.8 Main Simulations

There are three main simulations in this master's thesis which deals with: the erosion rate, the arc weld strength and the influence of changing material distribution of the layered model.

4.8.1   Erosion Rate – Amount of Eroded Material

The reason for examining the contact erosion, is to find the effects it has on the contacts during closing. Contact erosion creates a rough surface and may lead to unwanted heat generation in the closed position, resulting in contact melting. Hence, the mechanical and electrical properties decrease.

Figure 28 presents an example of contact erosion at the moving contact. Where the white zone between the fixed- and moving contact represents the area where contact erosion occurred. The first scale indicates the melting temperature of the contact material, which in this case is copper at 1358 K. The second scale shows the temperature gradient in the simulation, where the temperature increases along with the intensity from blue to red. Meaning that the blue colour indicates the coldest areas of the simulation and the red colour indicates the hottest.

Figure 28: Presents the contact erosion at the time of mechanical touch. The upper contact is the moving contact, while the lower one is the fixed contact. (1) Indicates the melting temperature of the contact material. (2) Indicates the temperature scale of the simulations.

49

4.8.2 Temperature Distribution – Arc Weld Strength

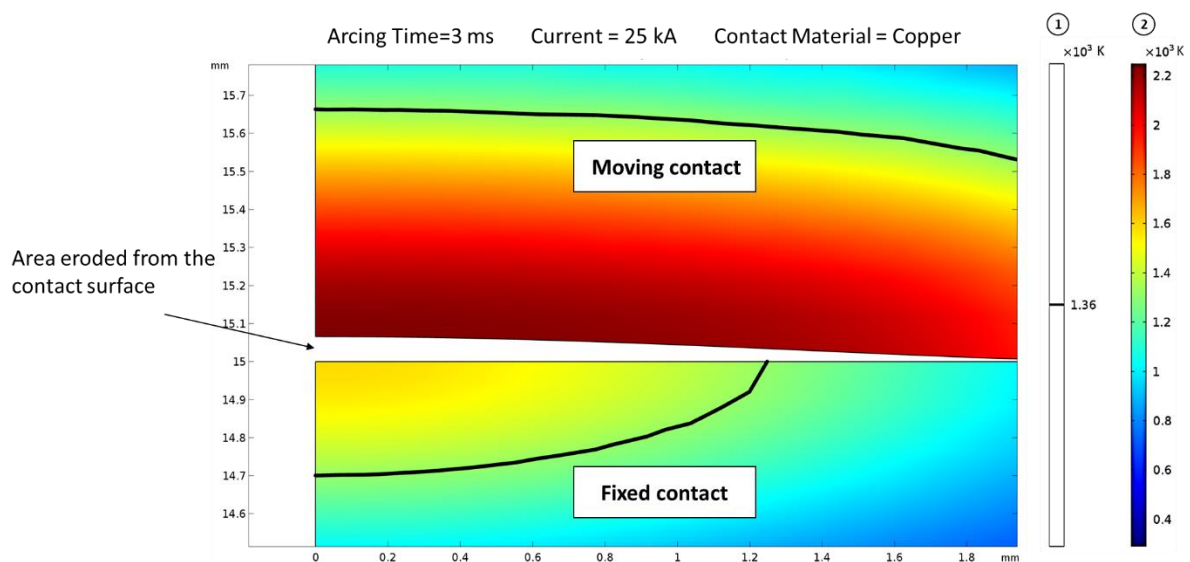The aim for examining temperature distribution, is the fear of contact welding. Contact welding influences the next breaking operation and can cause the switchgear to be unresponsive towards the opening command. As previously explained, arc welding is created when liquified contact material from both electrodes are in close proximity of each other. Hence, the liquidized material fuses together, cools down and creates a weld between the contacts.

There has not been implemented any fuse mechanism in the COMSOL model, therefore the welding properties was not fully simulated. The weld area was calculated after the simulations, by assuming that the liquidized contact material fused together at mechanical touch. The contact material had to be directly across each other in order to form an arc weld. As previously mentioned, the weld strength is calculated from the weld area and the ultimate tensile strength of the welded material. Table 8 presents the ultimate tensile strengths for both materials [23], [24].

Table 8: Ultimate tensile strength for copper and tungsten. This value is assumed constant for the entire master's thesis [23], [24].

Ultimate tensile strength of copper and tungsten			
	Copper	**Tungsten**	**Unit**
Tensile Strength	210	980	**[MPa]**

Figure 29 presents an example where arc welding is created between the fixed- and moving contact. The arc weld is represented by a gray box, to give a better visualisation of the welded area. The black lines defines the boundary between the solid and liquid contact material. From the figure, the arc weld is assumed to be created when the liquified contact material at the fixed- and moving contact is in close proximity to each other. In this example, the assumed arc weld radius was limited by the amount of liquified contact material at the fixed contact.
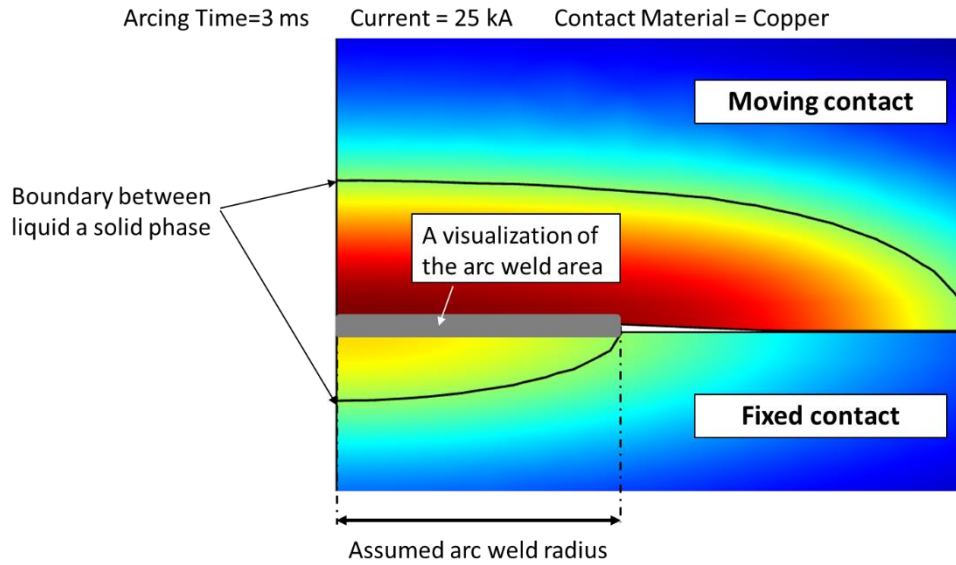
Figure 29: Presents the contact surface at the time of mechanical touch. The solid black line defines the boundary between the solid and liquid material. The gray box illustrates the assumed arc weld area.

4.8.3 Material Distribution in the Composite Material Copper-Tungsten.

The last main simulation dealt with the influence of changing material distribution of the layered model. It is possible to change the thickness of each layer when simulating the layered model. From experiments in a previous paper, melting and evaporation of the contact material depends on the distribution between the conductive and refraction material [6]. Hence, the grain size and material distribution influence the impacts a pre-strike arc has on the contact material. Two different material distributions were simulated: one with high copper density and one with high tungsten density. With a high copper density, the thickness of the copper layer was twice as for tungsten, and vice versa when the density of tungsten was high. This is presented in Table 9 and Figure 30.

Table 9: The geometrical dimensions used when simulating the change in material distribution.

Geomatical dimensions with change in material distribution		
	Copper	**Tungsten**
High copper density	1.666 mm	0.8333 mm
High tungsten density	0.833 mm	1.666 mm
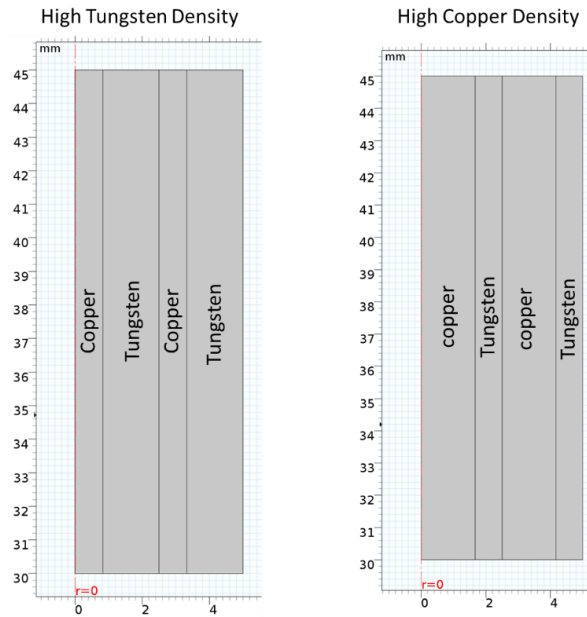
Figure 30: Illustration of the layered models simulated when the change in material distribution is examined.

4.9 Changing Parameters

There are two main parameters in this master's thesis: the short-circuit current flowing during arcing and the time period where the pre-strike arc is active.

4.9.1 Short-Circuit Current

There are upper short-current limits a switching device can brake during faults. This corresponds to the R10 series of Renard, based on the values proportional to $10^{\frac{n}{10}}$ (e.g. 10 kA, 15 kA, 20 kA, 25 kA, 31.5 kA, 40 kA, etc.). For medium voltage switchgears, these are 20 kA, 25 kA and 31.5kA. Therefore, these three values have been chosen as the varying parameters. The reason for examining the current level is to find the impacts it has on contact erosion and arc welding properties.

4.9.2 Arcing Time

The arcing period strongly depends on the contact material, the insulation gas and the arc current, and is normally in the range of 2-4 ms. In this thesis the arcing time has been set to 2 ms, 3 ms and 4 ms. The initiation of closing was set to be at t=0 and the mechanical touch at t=10 ms.

4.10 Assumptions

Due to the complexity of the simulation of an electrical arc and the erosion mechanism, some assumptions are implemented. These are listed below:

The first assumption; The arc is assumed to be a static arc, making the electrical- and thermal conductivity to be constant throughout the entire simulation.

The second assumption; The dissipated energy released from the pre-strike arc is converted into a heat source applied at the contact surface.

The third assumption; The arc voltage is held constant throughout the entire simulation. The voltage drop at the anode and cathode is set to be equal to 7.5 V and 17.5 V respectively. The voltage drop in the arc column is neglected due to the short distance of the contact gap.

The fourth assumption; No forced cooling is implemented to the contact. The only cooling implemented to the model is radiation cooling between the contact surface and the surroundings.

The fifth assumption; The composite material copper-tungsten is assumed to be layered.

The sixth assumption; All evaporation is considered as mass loss. This is considered the main erosion factor in all simulations.

The seventh assumption; The material properties are considered constant. It only changes during the phase change between solid and liquid state.

The eighth assumption; The arc weld is assumed to be present, when the melted material on the moving and fixed contact is in close proximity to each other.

The ninth assumption; The arc weld is assumed to be circular when calculating the arc weld force, in order to simplify the weld area calculation.

Chapter 5

Results from the Simulations

In this chapter, the simulated results are presented. The aim was to find the arc weld strength and the rate of contact erosion. First the contact erosion is presented, followed by the arc weld strength calculations. Last, the results from the changed material distribution is presented. For all three cases, the changing parameters was: short-circuit current, arcing time and contact material.

Results from each main simulation is organized based on the three arcing periods. For each subsection, the arcing period was held constant with only changing the short-circuit current and contact material.

5.1 Contact Erosion – Amount of Transported Contact Material

Vaporisation is considered the main reason for contact erosion in this master's thesis, meaning that the contact material evaporates and disappears when it exceeds the boiling temperature. As the geometry changes throughout the simulation, the material loss can be estimated at every time instance. Implying that it is possible to find the volume loss and mass loss of the contact material. Each curve presented has a time interval from 0 to 12 ms, as the heat flux needs time to move outwards in the geometry. This causes the temperature distribution to change after the pre-strike arc has quenched.

5.1.1   Arcing Time - 2 ms

This sub-chapter presents the amount of eroded contact material when the arcing time was 2 ms. Hence, the arc ignited 8 ms after the closing command was initiated. The short arcing period resulted in low amounts of heat dissipated and low contact erosion for all three contact materials. The contact material copper-tungsten had no contact erosion for all short-circuit current, hence no values are presented. Pure copper had contact erosion at short circuit currents 25 kA and 31.5 kA. While pure tungsten only had minor contact erosion for the short-circuit current 31.5kA. Contact erosion was only observed at the moving contact. Table 10 and Table 11 presents the results from the simulations with 2 ms as the arcing period. Figure 31 and Figure 32 shows a graph presenting the material loss for pure copper and tungsten.

Table 10: Material loss for pure copper when 2 ms arcing time was used.

Total material losses - Copper				
Short-Circuit Current	**Mass loss [mg]**		**Volume loss [mm³]**	
	Moving contact	**Fixed contact**	**Moving contact**	**Fixed contact**
20 kA	**0 mg**	**0 mg**	**0 mm³**	**0 mm³**
25 kA	**0.89 mg**	**0 mg**	**0.10 mm³**	**0 mm³**
31.5 kA	**2.68 mg**	**0 mg**	**0.30 mm³**	**0 mm³**
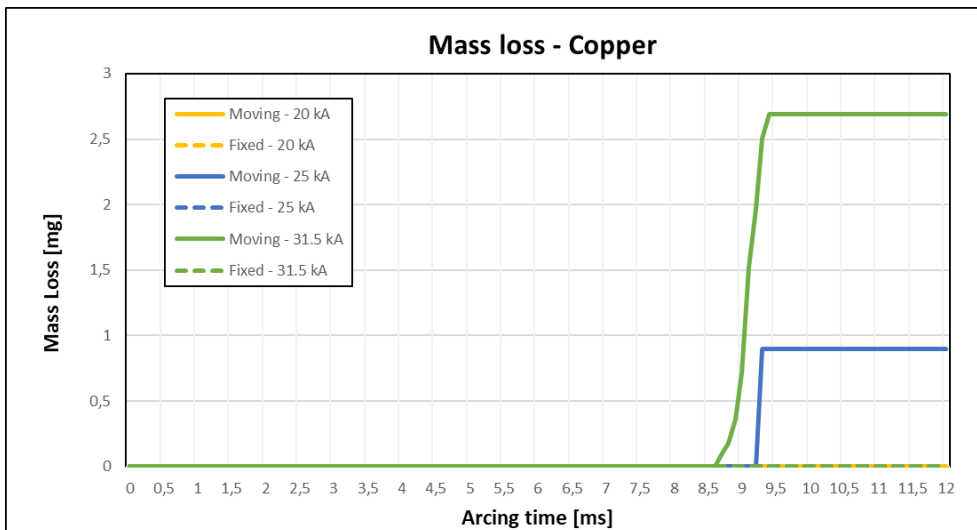
Figure 31: Mass loss of the contact when pure copper was used as the contact material. The solid lines describe the mass loss at the moving contact, while the dashed line describes the mass loss at the fixed contact. The time interval is 0 to 12 ms.

Table 11: Material loss for pure tungsten when 2 ms arcing time was used.

Total material losses - Tungsten				
Short-Circuit Current	**Mass loss [mg]**		**Volume loss [mm^3]**	
	Moving contact	**Fixed contact**	**Moving contact**	**Fixed contact**
20 kA	0 mg	0 mg	0 mm^3	0 mm^3
25 kA	0 mg	0 mg	0 mm^3	0 mm^3
31.5 kA	1.93 mg	0 mg	0.10 mm^3	0 mm^3

Figure 32: Mass loss of the contact when pure tungsten was used as the contact material. The solid lines describe the mass loss at the moving contact, while the dashed line describes the mass loss at the fixed contact.

Figure 33 to Figure 35 presents the three different contact materials at the time of mechanical touch with a short-circuit current of 31.5 kA. It can be observed that there is only a small amount of contact erosion when simulating the pure copper or tungsten. The contact erosion is in these cases presented at the left side of the pictures, i.e. at the centre of the arc column. When simulating the copper-tungsten, there is no material erosion. Figure 35 presents a contact when no contact erosion is present.
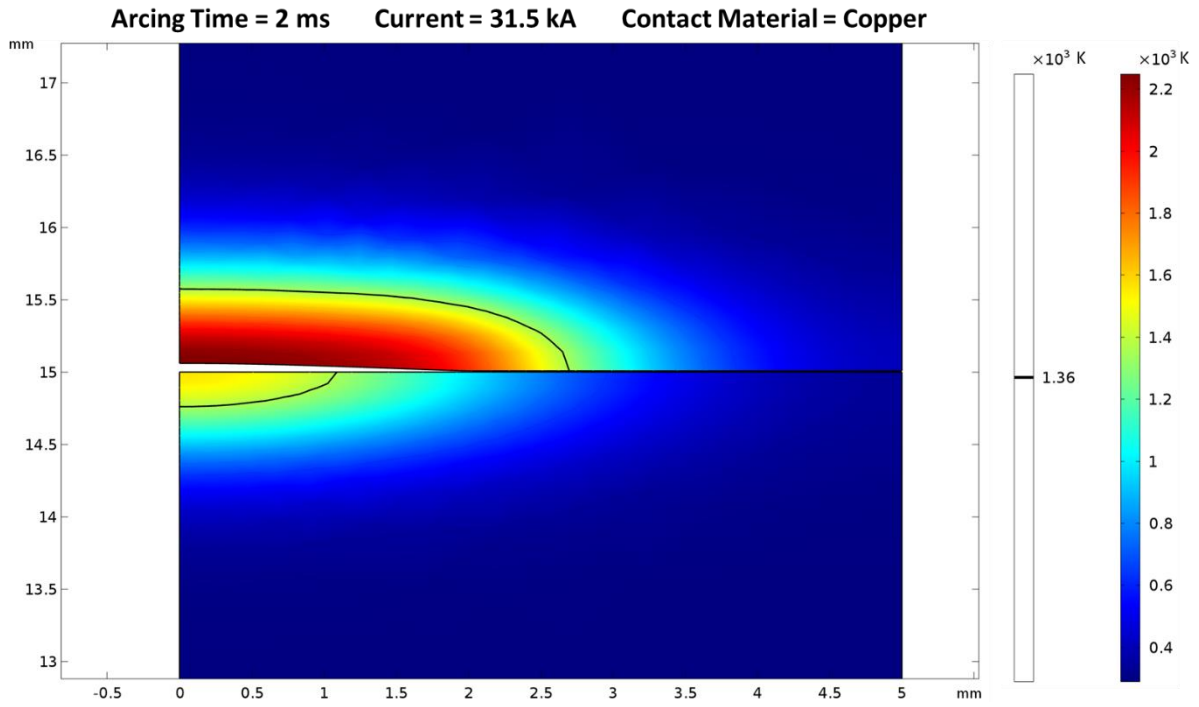
Figure 33: Presentation of contact erosion when pure copper was used as the contact material. The black line defines the boundary between the solid and liquid material.
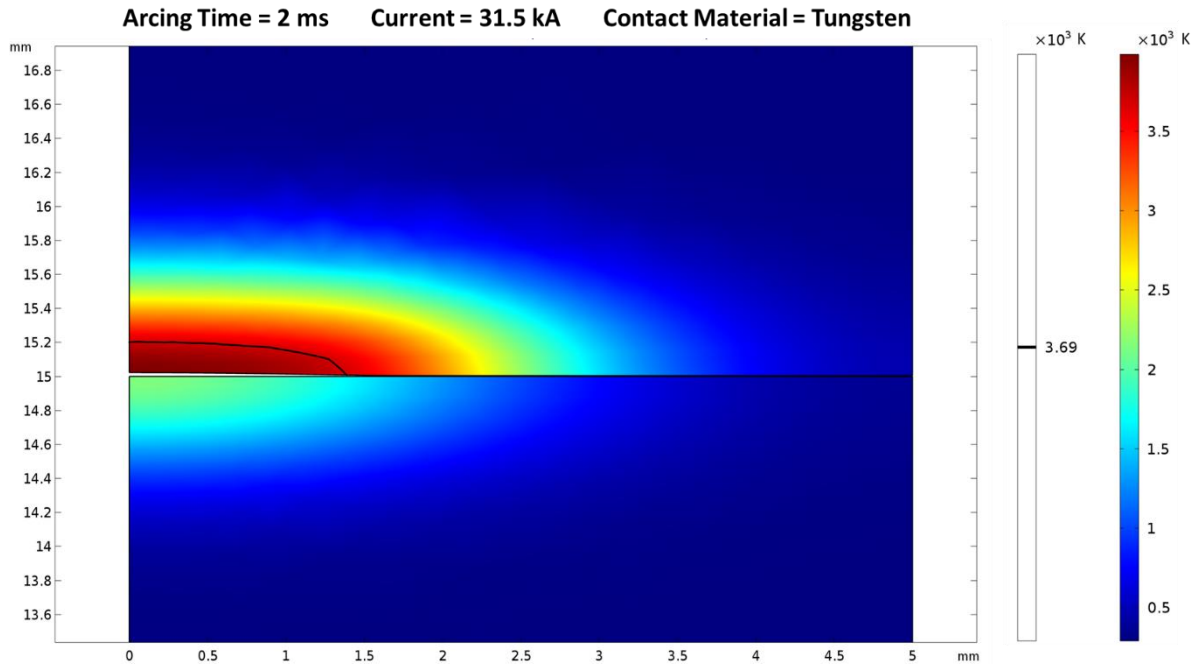
Figure 34: Presentation of contact erosion when pure tungsten was used as the contact material. The black line defines the boundary between the solid and liquid material.
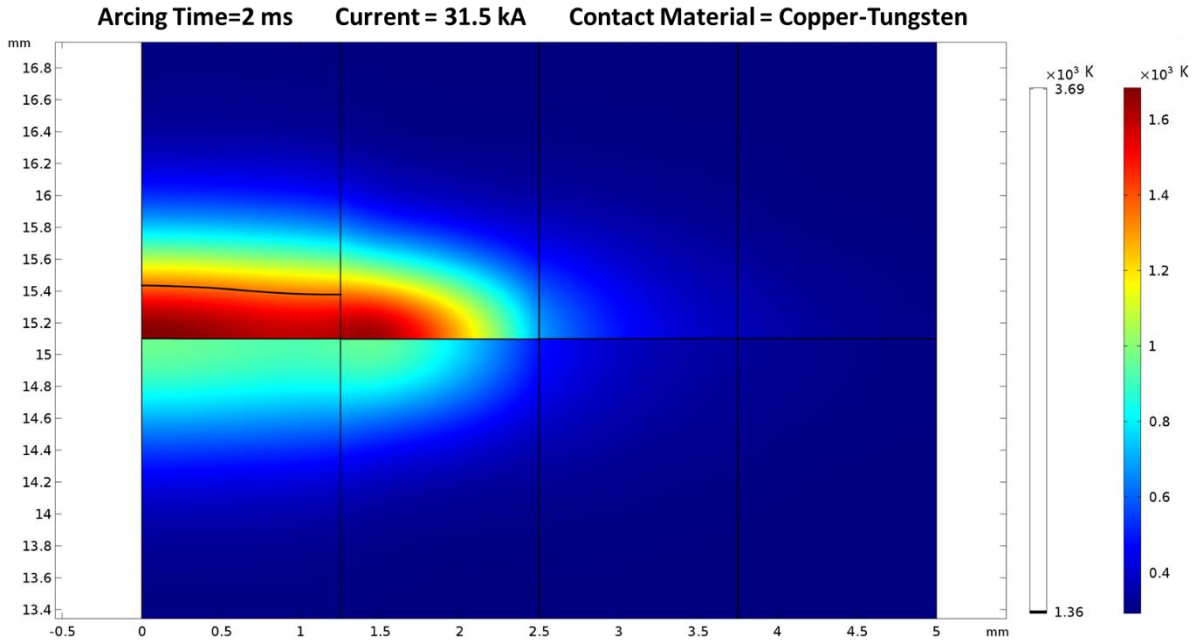
Figure 35: Presentation of contact erosion when copper-tungsten was used as the contact material. The black line defines the melting temperature of copper. The temperature does not exceed the melting temperature of tungsten, causing none of the tungsten particles to liquify.

5.1.2 Arcing Time - 3 ms

The arcing time for this sub-chapter was 3 ms. In this case the amount of eroded material on the moving contact, increased compared to the simulations with 2 ms arcing time. At this point, the amount of heat caused the copper-tungsten model to melt and evaporate, causing contact erosion. There is still no contact erosion on the fixed contact for all three cases, hence these values are not presented. Table 12 to Table 14 presents the contact erosion with 3 ms arcing time for each contact material. Figure 36 to Figure 38 presents the material loss for all three contact materials.

Table 12: Material loss for pure copper when 3 ms arcing time was used.

Total material losses - Copper				
Short-Circuit Current	**Mass loss [mg]**		**Volume loss [mm³]**	
	Moving contact	**Fixed contact**	**Moving contact**	**Fixed contact**
20 kA	**0.89 mg**	**0 mg**	**0.10 mm³**	**0 mm³**
25 kA	**2.68 mg**	**0 mg**	**0.30 mm³**	**0 mm³**
31.5 kA	**5.37 mg**	**0 mg**	**0.60 mm³**	**0 mm³**

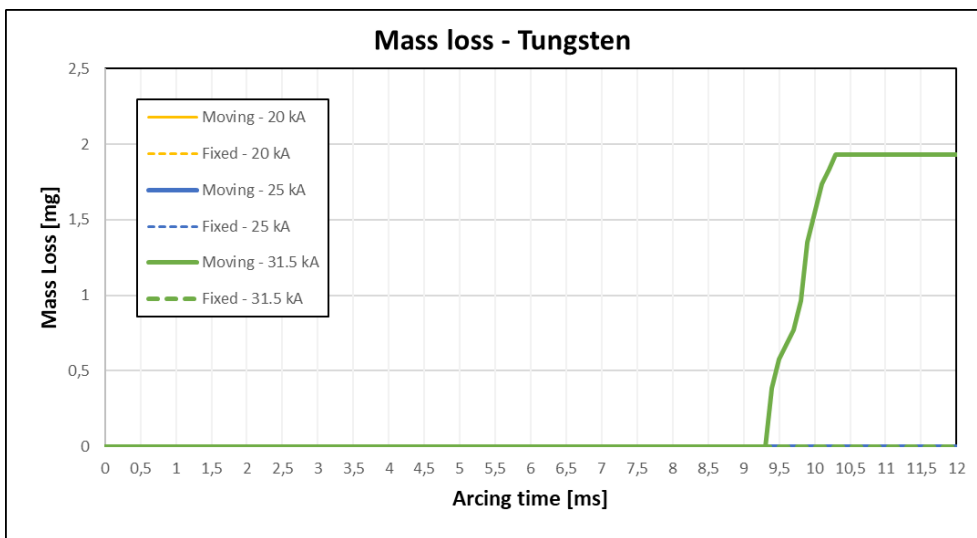*Figure 36: Mass loss of the contact when pure copper was used as the contact material. The solid lines describe the mass loss at the moving contact, while the dashed line describes the mass loss at the fixed contact.*

Table 13: Material loss for pure tungsten when 3 ms arcing time was used.

Total material losses - Tungsten				
Short-Circuit Current	**Mass loss [mg]**		**Volume loss [mm³]**	
	Moving contact	**Fixed contact**	**Moving contact**	**Fixed contact**
20 kA	**0 mg**	**0 mg**	**0 mm³**	**0 mm³**
25 kA	**1.93 mg**	**0 mg**	**0.10 mm³**	**0 mm³**
31.5 kA	**3.86 mg**	**0 mg**	**0.20 mm³**	**0 mm³**

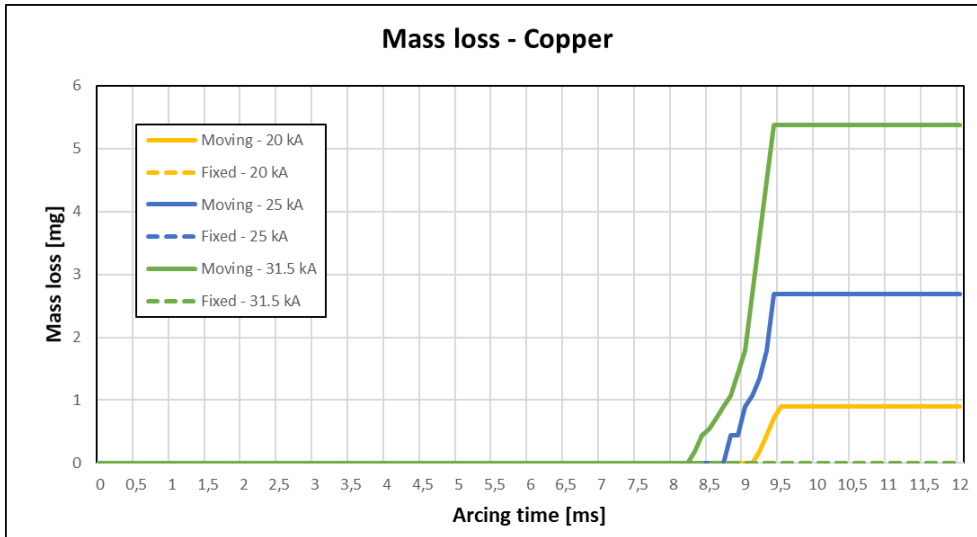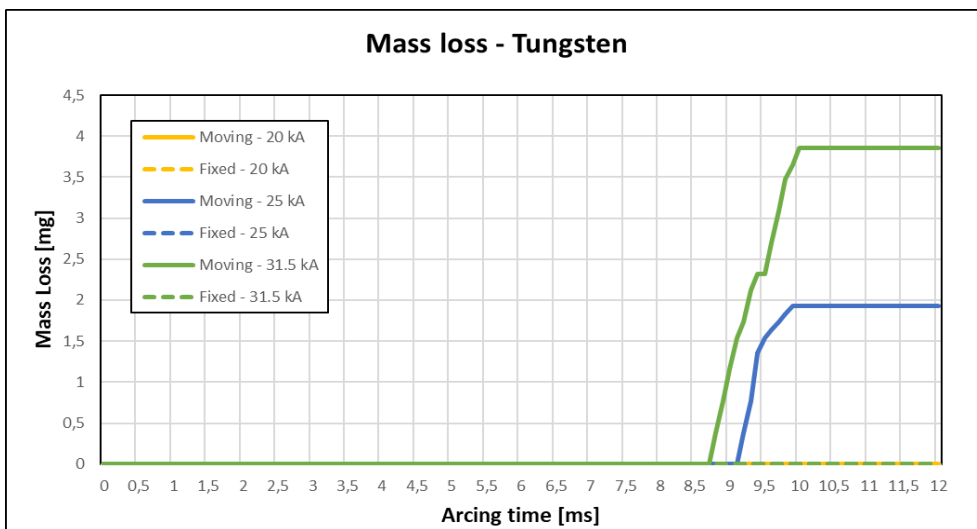*Figure 37: Mass loss of the contact when pure tungsten was used as the contact material. The solid lines describe the mass loss at the moving contact, while the dashed line describes the mass loss at the fixed contact.*

60

Table 14:Material loss for the moving contact when copper-tungsten was used. The arcing time was 3ms.

Total material losses of the moving contact - Copper-tungsten				
Short-Circuit Current	**Mass loss [mg]**		**Volume loss [mm³]**	
	Copper zones	**Tungsten zones**	**Copper zones**	**Tungsten zones**
20 kA	0.72 mg	0 mg	0.08 mm³	0 mm³
25 kA	1.7 mg	0.19 mg	0.19 mm³	0.10 mm³
31.5 kA	3.04 mg	0.39 mg	0.34 mm³	0.02 mm³
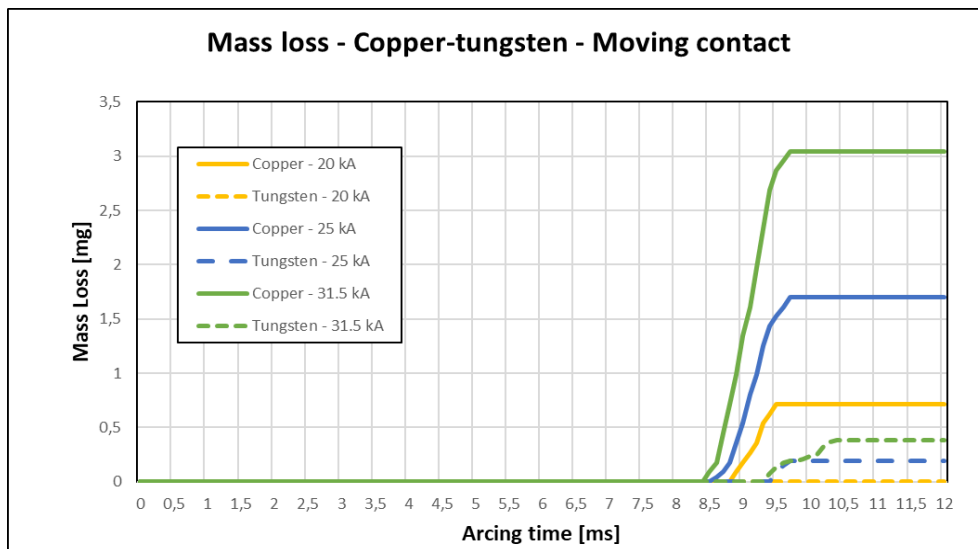
Figure 38: Mass loss of the moving contact when copper-tungsten was used. The solid lines describe the mass loss in the copper layer, while the dashed line describes the mass loss in the tungsten layer.

Figure 39 to Figure 41 presents the three contact materials at the time of mechanical touch with a short-circuit current of 31.5 kA. The pictures of the non-layered models have the same tendencies as those presented for 2 ms. Contact erosion occurs at the centre of the arc column.

The main noticeable change is observed in the layered-model copper-tungsten. Here, the highest amount of contact erosion occurs in two areas: in the centre of the arc column and at the boundary between the different material layers. Figure 41 presents a little crater at the boundary between the copper and tungsten layer. This crater is a result of the accumulated heat in the tungsten layer, caused by tungsten's low thermal conductivity. The low thermal conductivity causes the temperature in the tungsten layer to increase above the evaporation temperature of copper. Hence, the copper particles within near proximity of the tungsten layer melts and evaporates, creating the crater.
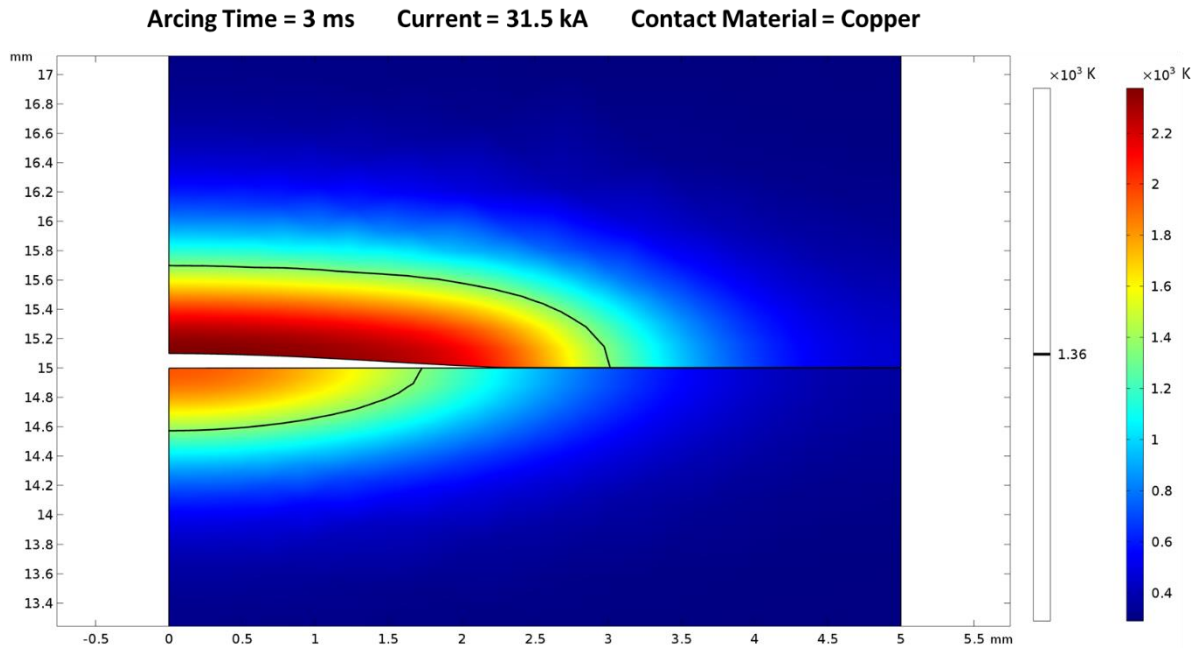
Figure 39: Presentation of contact erosion when pure copper was used as the contact material. The black line defines the boundary between the solid and liquid material.
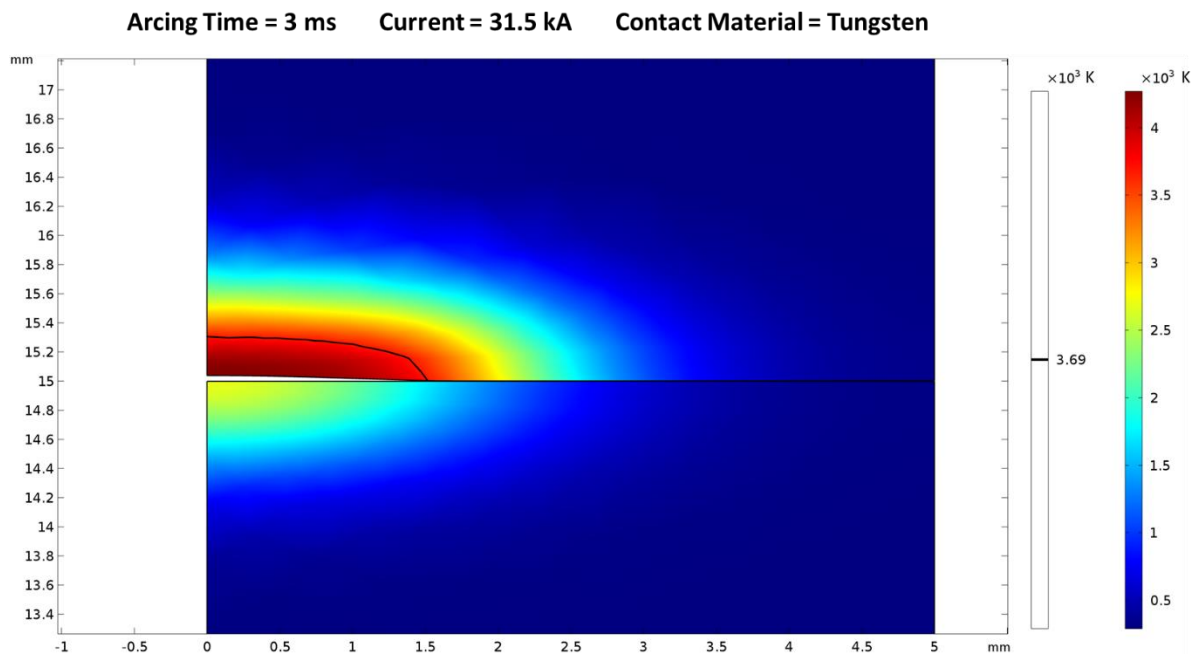
Figure 40: Presentation of contact erosion when pure tungsten was used as the contact material. The black line defines the boundary between the solid and liquid material.
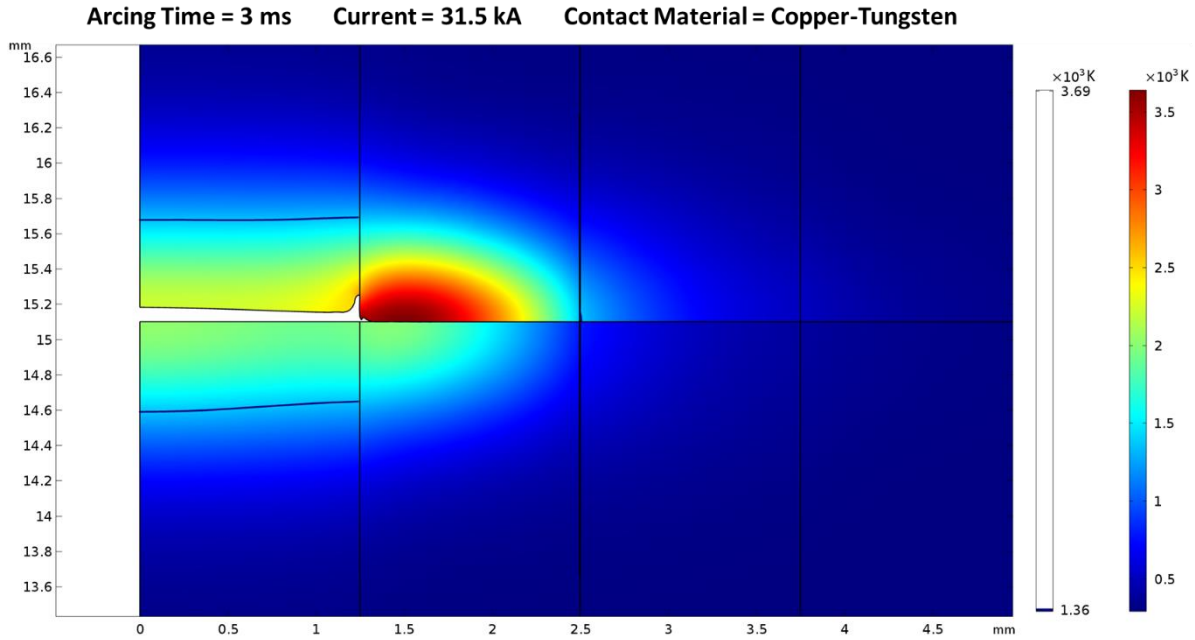
Figure 41: Contact erosion when copper-tungsten was the contact material. The black line defines the melting temperature of copper. A crater is present at the boundary between the first and second layer.

5.1.3 Arcing Time - 4 ms

The arcing time for this sub-chapter was 4 ms. The increased dissipated heat caused the fixed contact to melt, leading both of the contacts to be exposed for contact erosion. When the arcing time increased to 4 ms, the effect of the pre-strike arc begins to have some substantial impacts on the contact material. At this point, the amount of eroding material creates a big crater in the centre of the contact. Table 15 to Table 18 presents the contact erosion with 4 ms arcing time for each contact material. Figure 42 and Figure 43 presents the mass loss of the contact material consisting of pure copper or tungsten. The mass loss at the moving- and fixed contact in the copper-tungsten contact is shown in Figure 44 and Figure 45 respectively.

Table 15: Material loss for pure copper when 4 ms arcing time was used.

Total material losses - Copper				
Short-Circuit Current	**Mass loss [mg]**		**Volume loss [mm³]**	
	Moving contact	**Fixed contact**	**Moving contact**	**Fixed contact**
20 kA	9.85 mg	0 mg	1.1 mm³	0 mm³
25 kA	15.23 mg	0.89 mg	1.70 mm³	0.10 mm³
31.5 kA	24.19 mg	2.69 mg	2.70 mm³	0.30 mm³

Figure 42: Mass loss of the contact when pure copper was used as the contact material. The solid lines describe the mass loss at the moving contact, while the dashed line describes the mass loss at the fixed contact.

Table 16: Material loss for pure tungsten when 4 ms arcing time was used.

Total material losses - Tungsten				
Short-Circuit Current	Mass loss [mg]		Volume loss [mm^3]	
	Moving contact	Fixed contact	Moving contact	Fixed contact
20 kA	3.86 mg	0 mg	0.2 mm^3	0 mm^3
25 kA	9.65 mg	0 mg	0.5 mm^3	0 mm^3
31.5 kA	17.37 mg	0 mg	0.9 mm^3	0 mm^3

Figure 43: Mass loss of the contact when pure tungsten was used as the contact material. The solid lines describe the mass loss at the moving contact, while the dashed line describes the mass loss at the fixed contact.

64

Table 17: Material loss for the moving contact when copper-tungsten was used. The arcing time was 4 ms.

Total material losses of the moving contact - Copper-tungsten				
Short-Circuit Current	Mass loss [mg]		Volume loss [mm³]	
	Copper zones	Tungsten zones	Copper zones	Tungsten zones
20 kA	3.85 mg	0.38 mg	0.43 mm³	0.02 mm³
25 kA	5.82 mg	1.54 mg	0.65 mm³	0.08 mm³
31.5 kA	8.42 mg	4.24 mg	0.94 mm³	0.22 mm³
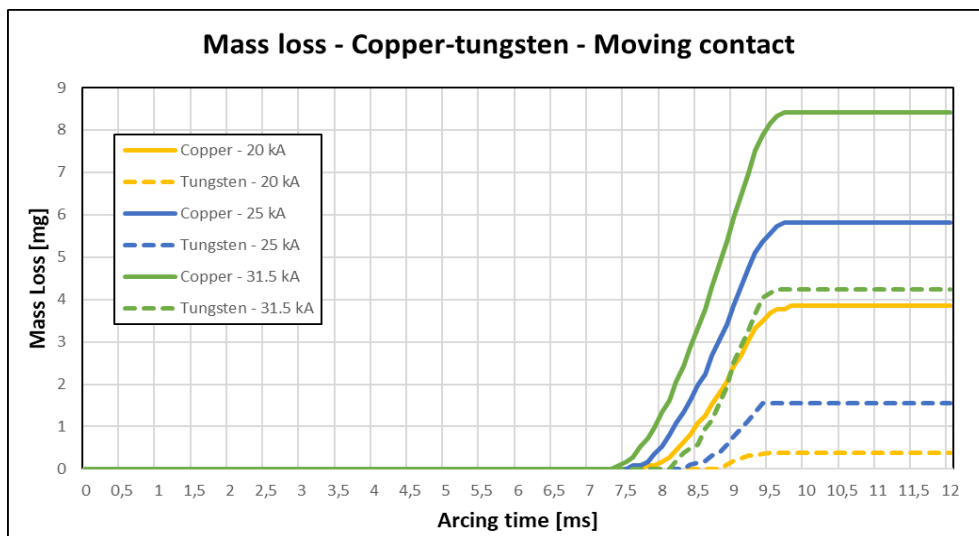
Figure 44: Mass loss of the moving contact when copper-tungsten was used as the contact material. The solid lines describe the mass loss in the copper layer, while the dashed line describes the mass loss in the tungsten layer.

Table 18: Material loss for the fixed contact when copper-tungsten was used. The arcing time was 4 ms.

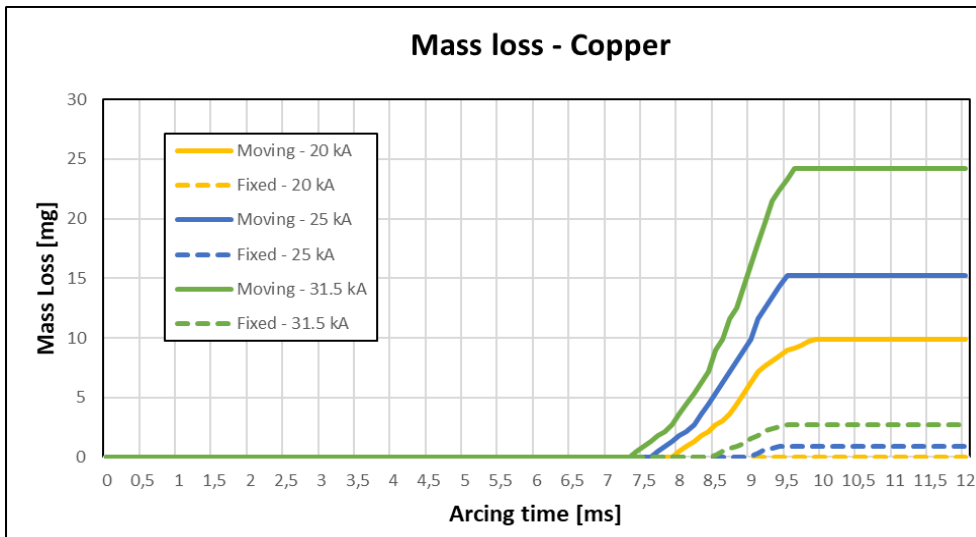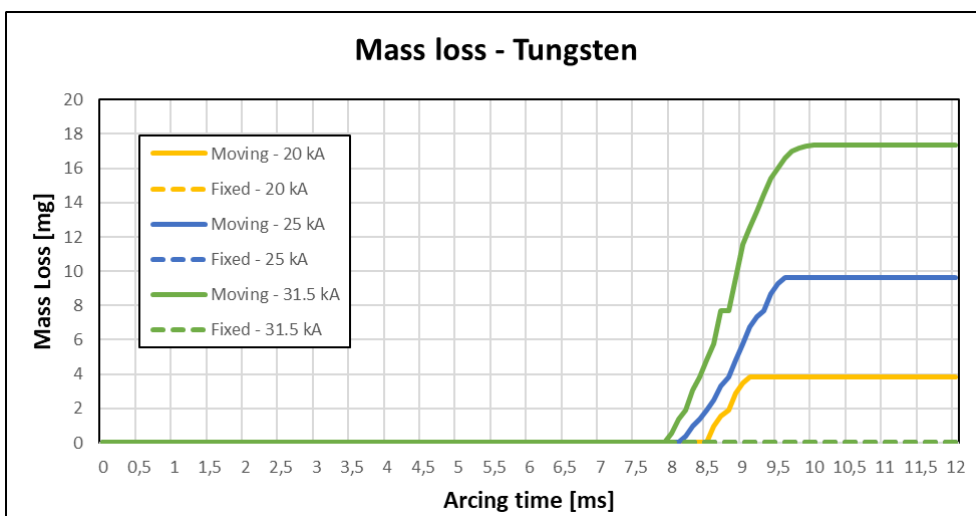| Total material losses of the fixed contact - Copper-tungsten				
Short-Circuit Current	Mass loss [mg]		Volume loss [mm³]	
	Copper zones	Tungsten zones	Copper zones	Tungsten zones
20 kA	0 mg	0 mg	0 mm³	0 mm³
25 kA	0.36 mg	0.58 mg	0.04 mm³	0.03 mm³
31.5 kA	1.25 mg	1.54 mg	0.14 mm³	0.08 mm³
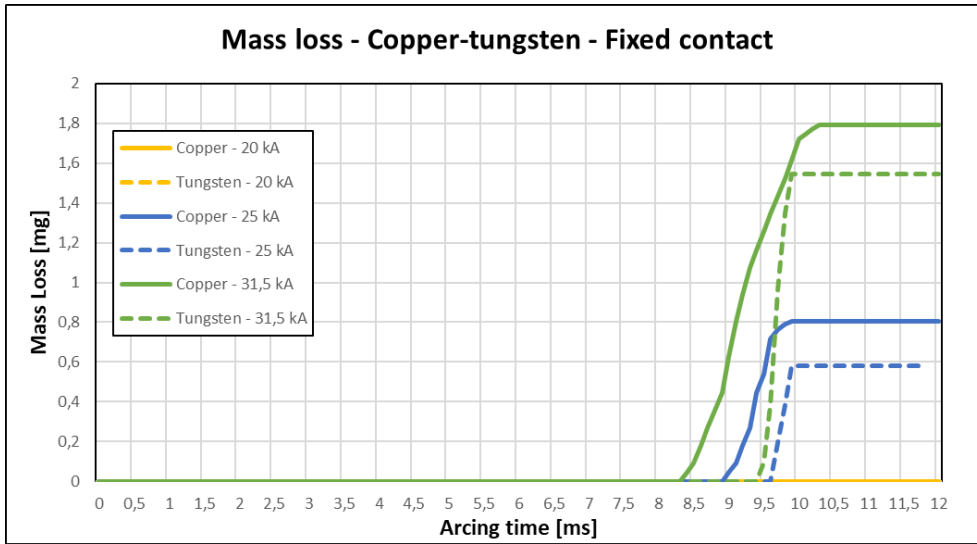
Figure 45: Mass loss of the fixed contact when copper-tungsten was used as the contact material. The solid lines describe the mass loss in the copper layer, while the dashed line describes the mass loss in the tungsten layer.

Figure 46 to Figure 48 presents the three contact materials at the time of mechanical touch with a short-circuit current of 31.5 kA. With longer arcing time, the fixed contact evaporates and contributes to the total amount of contact erosion. The same erosion tendencies for the non-layered model is present, with an increase in the amount of eroded material. Hence, the highest contact erosion is still at the centre of the arc column. For the copper-tungsten, the erosion crater phenomenon is present at both the fixed and moving contact.
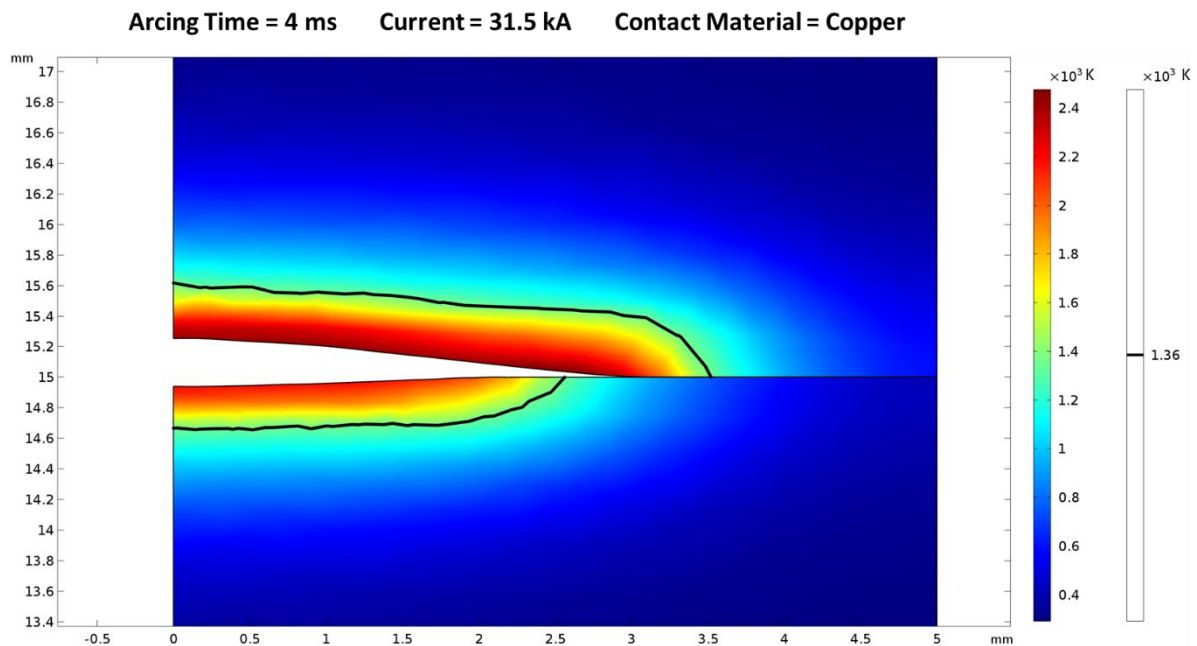
Figure 46: Presentation of contact erosion when pure copper was used as the contact material. The black line defines the boundary between the solid and liquid material.

66
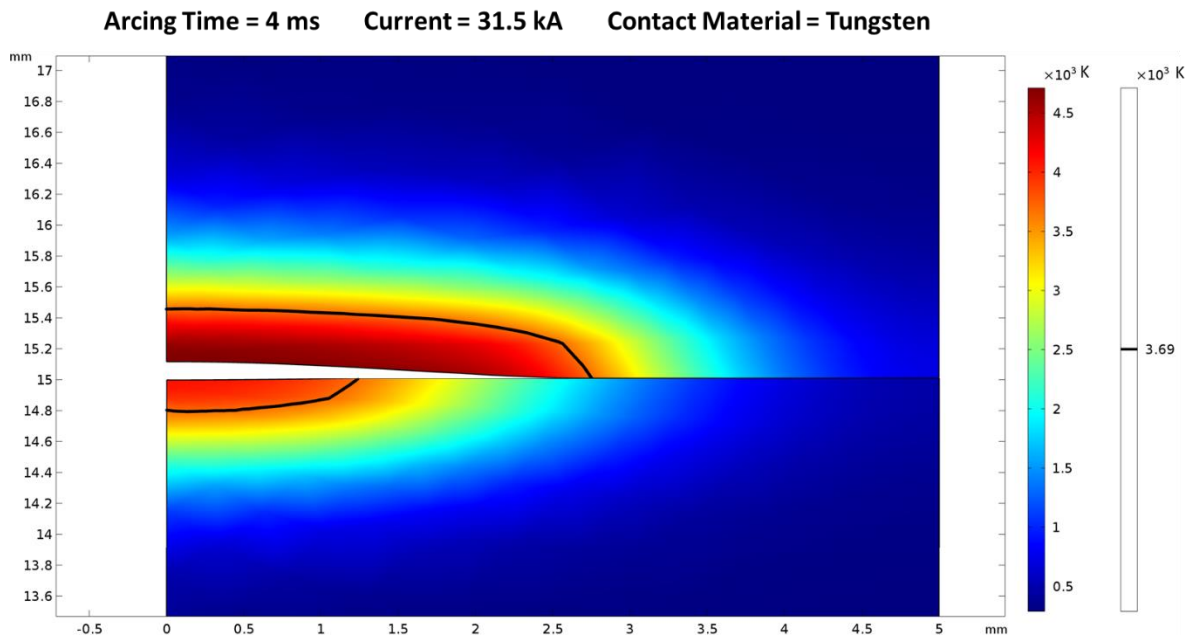
Figure 47: Presentation of contact erosion when pure tungsten was used as the contact material. The black line defines the boundary between the solid and liquid material.
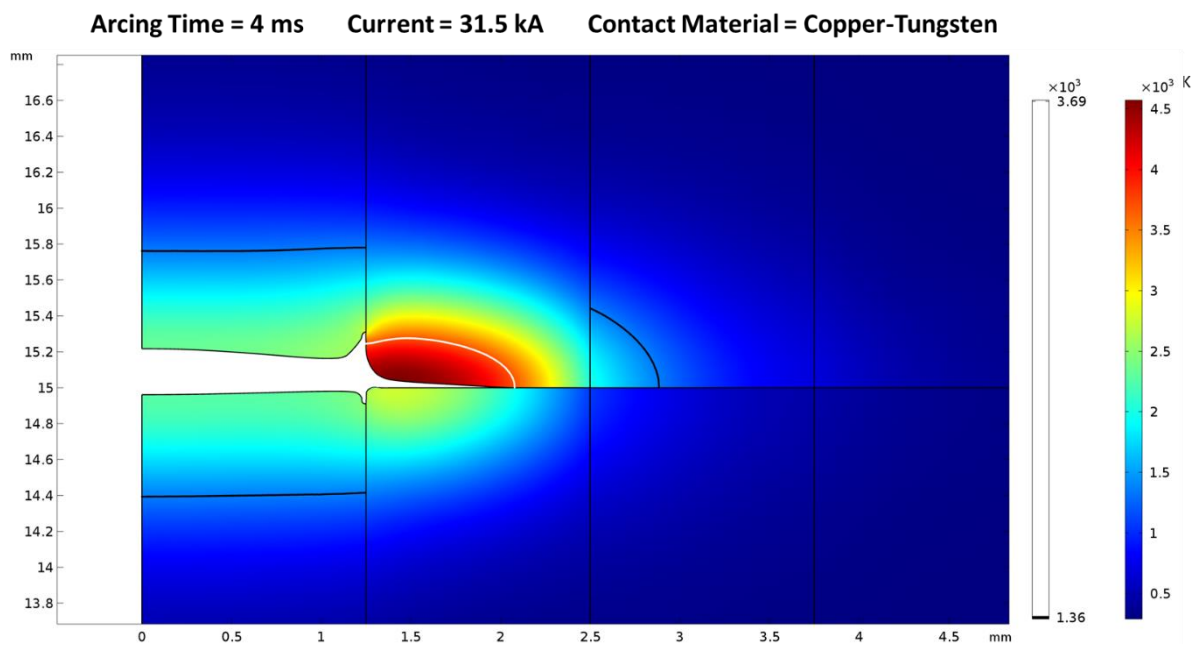
Figure 48: Contact erosion when copper-tungsten was the contact material. The black line defines the melting temperature of copper, while the white line defines the melting temperature of tungsten. A crater is present at both the fixed and moving contact between the first and second layer.

5.2 Arc Weld Strength – Temperature Distribution

Arc welding is considered as an unwanted phenomenon with regard to switching devices. One of the main aims in this master's thesis is to find the welding force generated after the pre-strike arc has quenched. This was performed by examining the contact surface at the point of mechanical touch.

The area of the arc weld is assumed to be where the liquidised material of the moving and fixed contact is in close proximity of each other. As fusing mechanisms was not implemented, the arc weld strength was calculated after the simulations. From chapter 3.5 *"Arc Welding – Concerns When Closing an Electrical Switching Device"*, the force required to break the weld depends on the weld area and the ultimate tensile strength of the contact material, as shown in Equation (3.3).

5.2.1 Arcing Time - 2 ms

For 2 ms arcing time, only one simulation indicated arc welding. This was the simulation with pure copper as the contact material, as it has a low melting temperature. Little energy is required to melt the pure copper contacts, causing a weld to be created at an early stage. The short-circuit current where copper started to weld was 31.5 kA. The welds strength is presented in Table 19.

Table 19: Arc weld strength when copper was used as the contact material. The arc welding is only present when the short-circuit current is equal to 31.5 kA.

Arc welding strength - Copper		
Short-Circuit Current	**Length of the weld (Diameter)**	**Arc weld strength**
20 kA	**0 mm**	**0 N**
25 kA	**0 mm**	**0 N**
31.5 kA	**2.2 mm**	**1596.5 N**

5.2.2 Arcing Time - 3 ms

Using 3 ms arcing time, the copper-tungsten model created a weld. The dissipated energy was high enough to melt the first copper layer at the fixed contact. Hence, a weld was created at the first copper layer between both contacts. The arc weld strength for copper-tungsten is presented in Table 20.

Table 20: Arc weld strength when copper-tungsten model was the contact material. Arc welding was only present in the first copper layer.

Arc welding strength – Copper-Tungsten		
Short-Circuit Current	**Length of the weld (Diameter)**	**Arc weld strength**
20 kA	**0 mm**	**0 N**
25 kA	**2.5 mm**	**2061.7 N**
31.5 kA	**2.5 mm**	**2061.7 N**

As for 2 ms arcing time, a weld was only created for the pure copper contact when examination the non-layered models. The simulations showed that the area of the arc weld increases with increased current. Table 21 presents the arc weld strength for pure copper.

Table 21: Arc weld strength when pure copper was used as the contact material.

Arc welding strength - Copper		
Short-Circuit Current	**Length of the weld (Diameter)**	**Arc weld strength**
20 kA	**0 mm**	**0 N**
25 kA	**2.5 mm**	**2084.8 N**
31.5 kA	**3.46 mm**	**3950.0 N**

5.2.3 Arcing Time - 4 ms

The simulation with pure tungsten started to create an arc weld when the arcing time increased to 4 ms. At this point, the increased dissipated energy causes the tungsten material to melt at the fixed contact. The weld created has a short diameter, but the weld strength is high. From the calculations, the pure tungsten weld requires a higher force to break the arc weld compared to pure copper. Table 22 and Table 23 presents the weld strength of the non-layered models.

Table 22: Arc weld strength when pure copper was used as the contact material.

Arc welding strength - Copper		
Short-Circuit Current	**Length of the weld (Diameter)**	**Arc weld strength**
20 kA	**3.9 mm**	**5017.3 N**
25 kA	**4.64 mm**	**7101.9 N**
31.5 kA	**5.1 mm**	**8580.0 N**

Table 23: Arc weld strength when pure tungsten was used as the contact material.

Arc welding strength - Tungsten		
Short-Circuit Current	**Length of the weld (Diameter)**	**Arc weld strength**
20 kA	**0 mm**	**0 N**
25 kA	**1.78 mm**	**4877.3 N**
31.5 kA	**2.5 mm**	**9621.1 N**

When copper-tungsten was simulated, only the first copper layer of the contacts welds together. For the first tungsten layer, the dissipated heat at the fixed contact was insufficient to increase the tungsten temperature above its melting temperature. Resulting in a constant weld area for all three short-circuit currents. Table 24 presents the weld strength when copper-tungsten was used as the contact material.

Table 24: Arc weld strength when copper-tungsten was used. Arc welding was only present at the first copper layer, resulting in a constant weld area.

Arc welding strength – Copper-Tungsten		
Short-Circuit Current	**Length of the weld (Diameter)**	**Arc weld strength**
20 kA	**2.5 mm**	**2061.7 N**
25 kA	**2.5 mm**	**2061.7 N**
31.5 kA	**2.5 mm**	**2061.7 N**

5.3 Material Distribution – Copper-Tungsten

The distribution of contact material is considered a factor impacting both the contact erosion and the arc-welding strength. As previously mentioned, an increase in copper particles at the contact, increases contact erosion and the arc weld strength. Conversely, increasing tungsten particles at the contact reduces contact erosion and arc weld strength, but contact resistance increases significantly.

In this section the results from both contact erosion and arc-weld strength with different material density is presented. Only 4 ms arcing time has been examined, in order to expose the contact material for the maximum thermal stresses. The short-circuit current was still varying between 20 kA, 25 kA and 31.5 kA.

5.3.1 Contact Erosion

Table 25 to Table 28 presents the values of contact erosion when the arcing time was 4 ms. It was observed that a high copper density caused a higher amount of material loss, than the contact with high tungsten density. This effect is related to the low vaporisation temperature of copper.

When examining the simulation with high tungsten density, the amount of tungsten particles evaporated is higher compared to copper. Since, the low thermal conductivity of tungsten causes an accumulation of heat and an increase in contact temperature.

Figure 49 and Figure 50 presents the mass loss of the moving- and fixed contact with high copper density respectively. Mass loss of the moving- and fixed contact with high tungsten density is presented in Figure 51 and Figure 52.

Table 25: Material loss for the moving contact when simulating with a high copper density.

Material losses of the moving contact – High copper density				
Short-Circuit Current	Mass loss [mg]		Volume loss [mm³]	
	Copper zones	Tungsten zones	Copper zones	Tungsten zones
20 kA	4.56 mg	0.19 mg	0.51 mm³	0.01 mm³
25 kA	7.88 mg	0.38 mg	0.88 mm³	0.02 mm³
31.5 kA	11.2 mg	0.77 mg	1.25 mm³	0.04 mm³

Figure 49: Mass loss of the moving contact with high copper density. The solid lines describe the mass loss in the copper zones, while the dashed lines describe the mass loss at the tungsten areas.

Table 26: Material loss for the fixed contact when simulating with a high copper density.

Material losses of the fixed contact – High copper density				
Short-Circuit Current	**Mass loss [mg]**		**Volume loss [mm³]**	
	Copper zones	**Tungsten zones**	**Copper zones**	**Tungsten zones**
20 kA	**0 mg**	**0 mg**	**0 mm³**	**0 mm³**
25 kA	**0.18 mg**	**0 mg**	**0.02 mm³**	**0 mm³**
31.5 kA	**0.98 mg**	**0.096 mg**	**0.11 mm³**	**0.005 mm³**

Figure 50: Mass loss of the fixed contact with high copper density. The solid lines describe the mass loss in the copper zones, while the dashed lines describe the mass loss at the tungsten areas.

72

Table 27: Material loss for the moving contact when simulating with a high tungsten density.

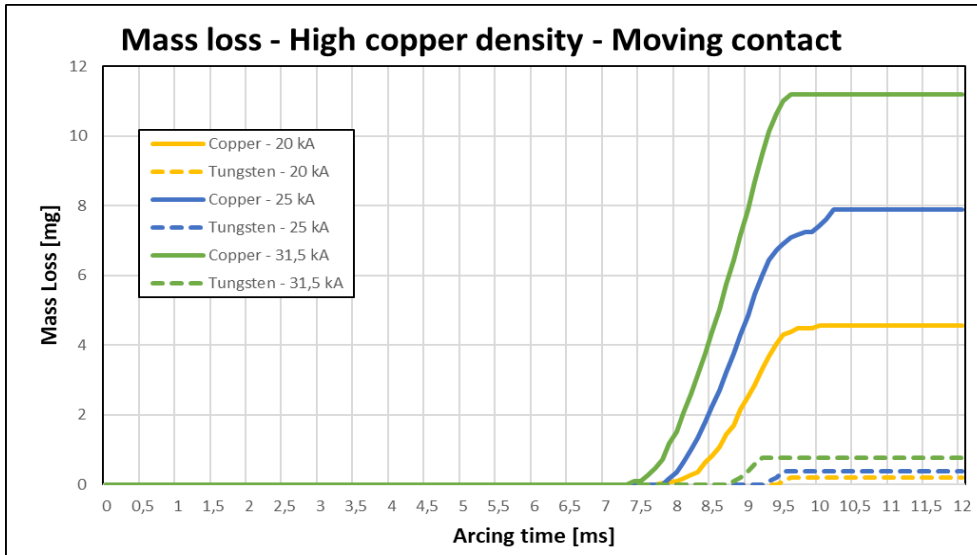| Material losses of the moving contact – High tungsten density				
Short-Circuit Current	**Mass loss [mg]**		**Volume loss [mm³]**	
	Copper zones	**Tungsten zones**	**Copper zones**	**Tungsten zones**
20 kA	1.88 mg	0.77 mg	0.21 mm³	0.04 mm³
25 kA	3.22 mg	3.47 mg	0.36 mm³	0.18 mm³
31.5 kA	4.48 mg	6.95 mg	0.5 mm³	0.36 mm³

Figure 51: Mass loss of the moving contact with high tungsten density. The solid lines describe the mass loss in the copper zones, while the dashed lines describe the mass loss at the tungsten areas.

Table 28: Material loss for the fixed contact when simulating with a high tungsten density.

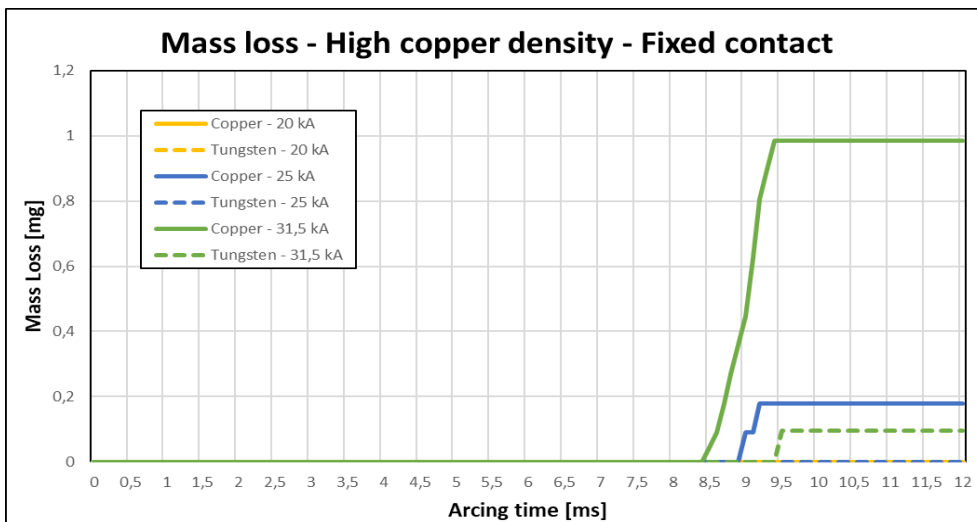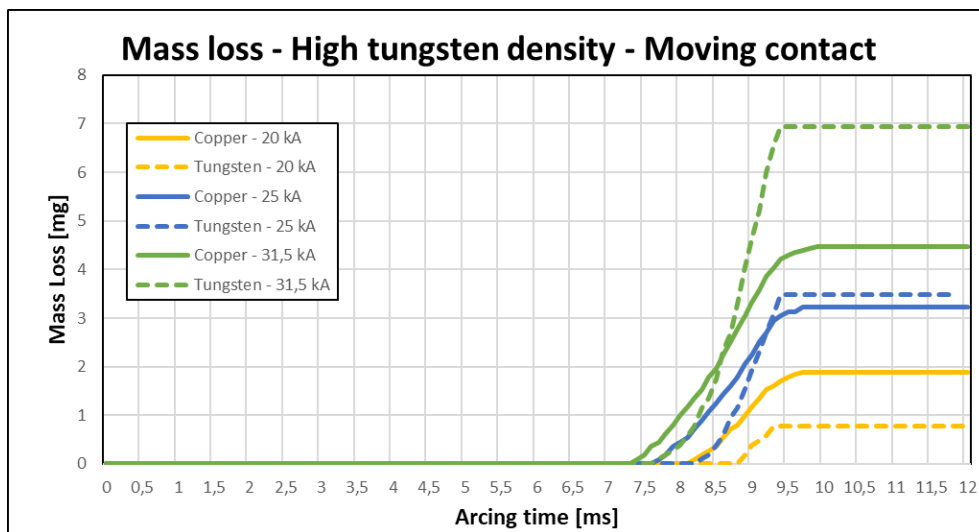| Material losses of the fixed contact – High tungsten density				
Short-Circuit Current	**Mass loss [mg]**		**Volume loss [mm³]**	
	Copper zones	**Tungsten zones**	**Copper zones**	**Tungsten zones**
20 kA	0.09 mg	0 mg	0.01 mm³	0 mm³
25 kA	0.36 mg	0 mg	0.04 mm³	0 mm³
31.5 kA	0.89 mg	0.19 mg	0.10 mm³	0.01 mm³

73
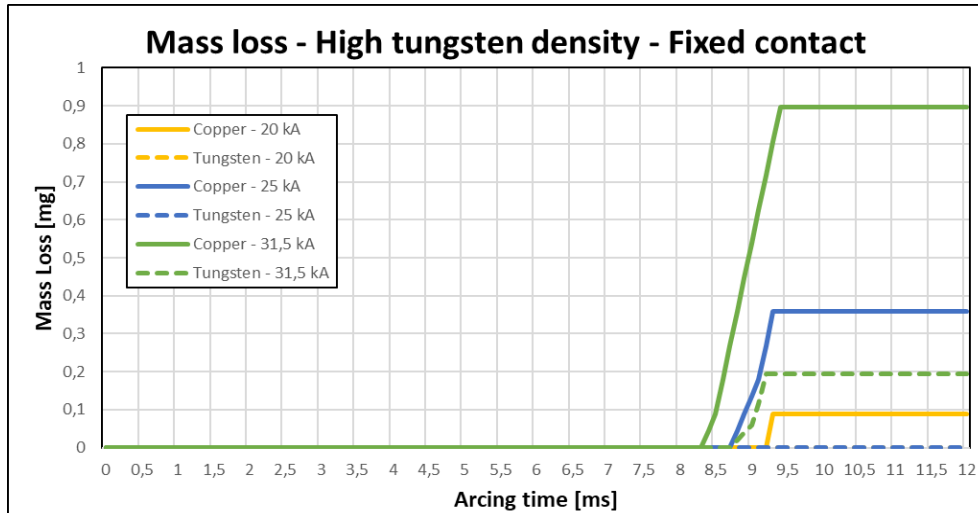
Figure 52: Mass loss of the fixed contact with high tungsten density. The solid lines describes the mass loss in the copper zones, while the dashed lines describes the mass loss at the tungsten areas.

Table 29 presents the total mass and volume loss for the contacts with 4 ms arcing time. It shows, the total mass- and volume loss regardless of the material zone. This implies that it includes the material losses of tungsten and copper at the moving and fixed contact.

Table 29: Presentation of the total mass and volume loss for both material distributions. The total mass and volume loss include the material losses of tungsten and copper at the moving and fixed contact.

Total material loss for both cases				
Short-Circuit Current	**High copper density**		**High tungsten density**	
	Volume loss	**Mass loss**	**Volume loss**	**Mass loss**
20 kA	0.52 mm^3	4.75 mg	0.26 mm^3	2.74 mg
25 kA	0.92 mm^3	8.44 mg	0.58 mm^3	7.05 mg
31.5 kA	1.405 mm^3	13.05 mg	0.97 mm^3	12.51 mg

5.3.2 Temperature distribution – Arc Welding

Figure 53 and Figure 54 presents the temperature distribution for both material distributions at the point of mechanical touch. It was not observed melting of the tungsten layer on the fixed contact at the point of mechanical touch. Hence, no arc welding was created between the first tungsten layers. Therefore, the amount of copper in the first layers has a major influence on the total weld area. Implying that the arc weld is longer with a high copper density, compared to the arc weld created with high tungsten density.
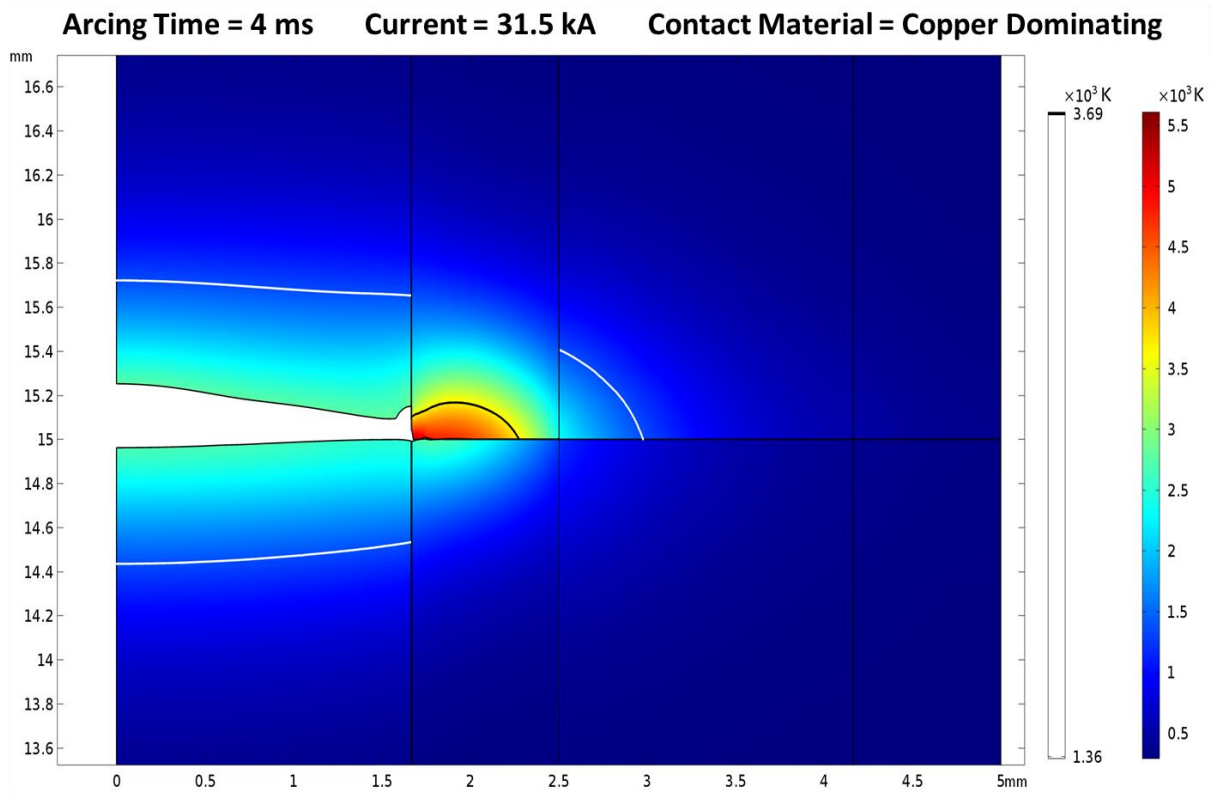
Figure 53: Temperature distribution of the contact with high copper density. The white line indicates the melting temperature of copper, while the black line indicates the melting temperature of tungsten.
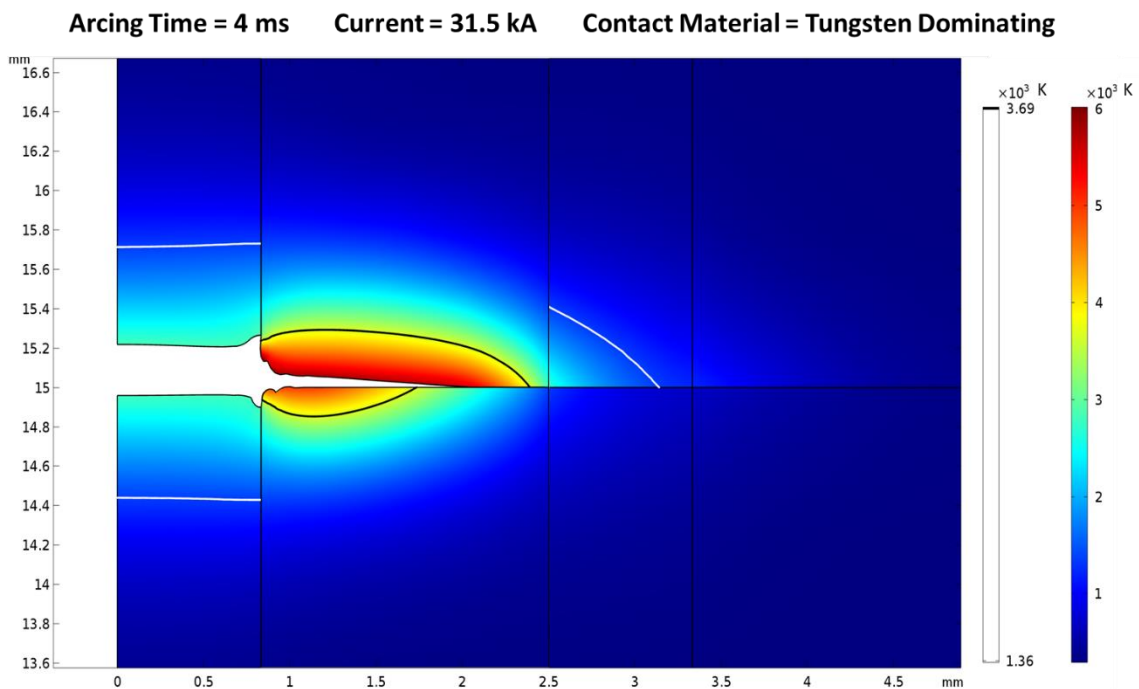
Figure 54: Temperature distribution of the contact with high tungsten density. The white line indicates the melting temperature of copper, while the black line indicates the melting temperature of tungsten.

75

Table 30 and Table 31 presents the arc weld strength for both contact distributions. The arc weld area and strength, for both contact distributions, was constant for all short-circuit currents.

Table 30: Arc weld strength for the contacts with high copper density.

Arc welding strength – High copper density		
Short-Circuit Current	**Length of the weld (Diameter)**	**Arc weld strength**
25 kA	1.666 mm	3662.2 N
25 kA	1.666 mm	3662.2 N
31.5 kA	1.666 mm	3662.2 N

Table 31: Arc weld strength for the contacts with high tungsten density.

Arc welding strength – High tungsten density		
Short-Circuit Current	**Length of the weld (Diameter)**	**Arc weld strength**
25 kA	0.833 mm	916.2 N
25 kA	0.833 mm	916.2 N
31.5 kA	0.833 mm	916.2 N

Chapter 6

Discussion

As previously explained, there are four states for a switching device: open position, closed position and the transition stages, opening and closing. In this thesis, the focus has been on the transition stage closing. To examine the quality of a switching device, three main stresses needs to be taken into consideration. These are: the mechanical-, dialectical- and thermal stresses.

Within the scope of this thesis, only thermal stresses have been examined. Hence, one cannot judge the entire quality of the contact material in the switching devices, only the influence thermal stresses had on the contact material.

This chapter will reflect around four main discussion points. First the advantages and disadvantages around the layered and non-layered models. Followed by the effect of changing the material distribution of the contact material copper-tungsten, and a discussion about the impacts caused by short circuit currents and arcing time. The chapter concludes with a discussion about the validity of the results.

6.1 Advantages and Disadvantages of the Layered and Non-Layered Model

The contact material examined in this thesis was pure copper and tungsten and the composite material copper-tungsten. Based on the FEM-models made in COMSOL, copper-tungsten had a lower arc weld strength and contact erosion, than pure copper and tungsten. It

was observed that the heat stresses generated from the pre-strike arc was better distributed when the contact material consisted of a conductive and refractory material. Hence, when examining the contact erosion and arc weld strength separately, the advantage of choosing copper-tungsten is more evident.

6.1.1 Contact Erosion

When examining contact erosion for the three contact materials, pure copper was the most exposed out of them, as seen in Table 32. Pure copper had the highest mass and volume loss for all three arcing times and short-circuit currents. This is directly connected to the low melting- and evaporation point of copper. Pure tungsten requires a higher amount of dissipated heat to melt and evaporate compared to pure copper. Therefore, the contact consisting of pure copper had more contact erosion compared to the one with pure tungsten.

Table 32: The total amount of contact erosion for the three contact materials. Each value is the total amount of lost material from both the moving- and fixed contact. Each value is given in milligrams (mg).

	Total material loss [mg]								
	2 ms			3 ms			4 ms		
	Pure Copper	Pure Tungsten	Copper-Tungsten	Pure Copper	Pure Tungsten	Copper-Tungsten	Pure Copper	Pure Tungsten	Copper-Tungsten
20 kA	0	0	0	0.89	0	0.72	9.85	3.86	4.23
25 kA	0.89	0	0	2.68	1.93	1.89	16.12	9.65	8.30
31.5 kA	2.68	1.93	0	5.37	3.86	2.82	26.88	17.37	15.45

For the layered simulation of copper-tungsten, the thermal stresses were shared between the different layers. Copper has a higher thermal conductivity than tungsten, causing the heat present in the copper zones to transfer to the tungsten zones. Additionally, since tungsten has a higher melting and evaporation point than copper, it can absorb more heat before it starts to deform (i.e. melts and/or evaporates). Thus, the thermal withstanding strength increases with the layered model, causing less contact erosion. Section 2.2.1 *"Materials Used in Switching Devices"* presented that by using a refractory metal (e.g. tungsten), the amount of contact wear decreases. This effect was observed in the results, where the layered model had lower contact erosion than the non-layered models.

With regard to contact erosion, the layered model consisting of copper-tungsten performed best towards the thermal stresses. A possible explanation is that the heat flux at the contacts could be transported between the material layers, creating a better heat distribution. This heat flux distribution was less effective when the contact contained pure copper or pure tungsten, since it only had one large continuous material layer.

6.1.2 Arc Weld Strength

Based on the calculations, the arc weld strength strongly depended on melting of the fixed contact, since the moving contact melted in all cases. Hence, the melting of the fixed contact was the main limitation in order to create a weld. From the simulations, pure copper was the weakest contact material with regard to arc welding. The copper present at the fixed contact, melted at a lower dissipated heat compared to the other contact materials (i.e. pure tungsten and copper-tungsten). The results was a larger weld cross-section in pure copper compared to the other contact materials. Further, the contact consisting of pure copper had a high weld strength at low short-circuit currents and short arcing time.

When examining pure tungsten, no arc-welding was created when the arcing time and short-circuit current were low. With high short-circuit current and arcing time, both the moving- and fixed contact melted, creating a strong weld. This is related to the high melting point of tungsten. At high currents and arcing time, the weld strength for pure tungsten is higher than pure copper, even though the weld area for tungsten is smaller. This is directly related to the ultimate tensile strength for both materials, as tungsten has an ultimate tensile strength four times higher than copper.

The weld strength for a copper-tungsten contact material, strongly depends on the density of copper particles at the fixed contact. It was observed that only copper melted at the fixed contact, when simulating the layered model. Thus, only the copper layer fused together and created a weld. The temperature at the fixed contact were not high enough to melt the tungsten layer on the fixed contact. Consequentially, the weld area was constant as only the first copper layer at both contacts melted and created a weld. Table 33 presents the weld strength for all three contact materials.

Table 33: The arc weld strength for all three contact materials. Each value presents the force needed to break the weld between the moving- and fixed contact. Each value is given in newtons (N)

	Arc welding strength [N]								
	2 ms			3 ms			4 ms		
	Pure Copper	Pure Tungsten	Copper-Tungsten	Pure Copper	Pure Tungsten	Copper-Tungsten	Pure Copper	Pure Tungsten	Copper-Tungsten
20 kA	0	0	0	0	0	0	5017.3	0	2061.7
25 kA	0	0	0	2084.8	0	2061.7	7101.9	4877.3	2061.7
31.5 kA	1596.5	0	0	3950	0	2061.7	8580	9621.1	2061.7

With regard to arc welding, the pure tungsten model was best with a low short-circuit current and arcing time. However, it performed the worst when the arcing time increased to 4 ms. Altogether, the copper-tungsten model performed the best on average. A possible explanation for why copper-tungsten is best towards arc welding, is that the first tungsten layer at the fixed contact acts as a limiting factor and prevents the weld area from increasing.

6.1.3 Advantages and Disadvantages with Copper-Tungsten

Copper-tungsten performed the best to both contact erosion and arc weld strength. It distributed the thermal stresses better than a contact consisting of only one material. The tungsten particles accumulated most of the heat generated from the pre-strike arc, causing the amount of evaporated material and area of liquified material to decrease. While the copper particles have a low contact resistance, causing it to conduct the current better when in closed position. By combining these materials in a contact, a material is created with high contact wear from tungsten and low contact resistance from copper. Therefore, a composite material like copper-tungsten are the favourable contact material in switching devices based on the thermal stresses.

The main disadvantage when using copper-tungsten and other composite materials, is the creation of uneven surfaces after several making and breaking operations. Over time, the amount of conductive material decreases due to contact erosion. Hence, there will be a reduction in contact points and increased thermal stresses on the contacts in the closed position. It is likely that most of the copper at the contact surface would evaporate, causing the surface to be less conductive, as tungsten has a high contact resistance.

6.2 Influence of Material Distribution in the Copper-Tungsten Model

Observations implies that copper and tungsten distribution had an effect on contact erosion and arc weld strength, when examining copper-tungsten. In this section, the influence of high copper density and high tungsten density is discussed, with regard to contact erosion and arc weld strength.

6.2.1 Contact Erosion

The difference in mass loss (mg), when considering the change in material distribution was marginal. For all three short-circuit currents, the mass loss was slightly higher when simulating high copper density. The difference was more apparent when examining the volume loss (mm^3), as presented in Table 34. When considering volume loss, the simulations with high copper density had a significantly higher loss compared to simulations with high tungsten density. An explanation is the large difference in material density between copper and tungsten. Tungsten has a material density of 19 300 kg/m^3, while copper has a material density of 8960 kg/m^3. In simulations with high copper density, the eroded material mostly contained copper particles. While in simulations with high tungsten density, the eroded material contained a mixture of both copper and tungsten particles.

Table 34: Total material loss for the contacts with high copper density and high tungsten density. The total mass and volume loss includes the material losses of tungsten and copper at the moving and fixed contact.

Total material loss for both cases				
Short-Circuit Current	**High copper density**		**High tungsten density**	
	Volume loss	**Mass loss**	**Volume loss**	**Mass loss**
20 kA	0.52 mm^3	4.75 mg	0.26 mm^3	2.74 mg
25 kA	0.92 mm^3	8.44 mg	0.58 mm^3	7.05 mg
31.5 kA	1.405 mm^3	13.05 mg	0.97 mm^3	12.51 mg

The best material distribution against contact erosion cannot be determined based on the results from mass loss. When considering the volume loss, high tungsten density performs better, as the total volume loss is smaller. In total, the model with high tungsten density had a better performance considering contact erosion. A possible explanation is that tungsten absorbs most of the heat, causing lower amounts of copper erosion in the high tungsten density model. In the high copper density model, the amount of tungsten present at the contacts is too low to absorb enough of the heat, causing copper to take most of the thermal stresses, i.e. more copper particles evaporate.

6.2.2 Arc Weld Strength

When considering the layered model, arc welding was closely related to the amount of copper particles at the fixed contact. Arc welding was only observed in the first copper layers, as copper melted at both the fixed and moving contact. Tungsten did not melt at the fixed contact, as it was not exposed for enough heat flux in order to melt. The total weld area was larger for the high copper density contacts, compared to the high tungsten density contacts. This is related to the amount of copper particles present in the contacts.

When examining the first copper layer of the fixed contact, it was observed that all copper particles melted at the contact surface, for all three short-circuit currents. Resulting in a constant weld area and weld strength for each model. When calculating the weld strength, the influencing factors are the weld area and ultimate tensile strength of the welded material (Equation (3.3)). For both models, the weld strength is only influenced by the weld area, as the ultimate tensile strength is constant for copper. Thus, the weld strength is constant for all short-circuit currents, as presented in Table 35.

Table 35: Arc weld strength for both cases when the arcing time was 4 ms.

Arc weld strength		
Short-Circuit Current	**High copper density**	**High tungsten density**
20 kA	**3662.2 N**	**916.2 N**
25 kA	**3662.2 N**	**916.2 N**
31.5 kA	**3662.2 N**	**916.2 N**

The values generated from the simulations are a bit misleading, since it presents a constant value for all short-circuit currents within both models. This is an effect of the coarse material distribution of the contacts, as the layered models is a simplification of a real contact. The weld strength would most likely be more realistic, if the contacts were built up by cubes instead of layers. With a cubical distribution, the weld area would most likely change along with a change in short-circuit current.

However, there is still some knowledge that can be gained from the layered models simulated in this thesis. The simulations indicate that only copper particles welds at the layered contacts. Furthermore, the arc weld strength increases with decreasing tungsten density. This supports what was presented in the theory about contact materials, that refractory materials decreases contact welding and wear.

6.2.3 Comparing the High Copper Density and High Tungsten Density

It was observed that both contact erosion and arc weld strength were lower when using high tungsten density contacts. This is directly related to the high wear resistance of tungsten. Unfortunately, this comes with a price. With an increased amount of tungsten particles at the contacts, the contact resistance increases and more thermal stresses is generated in closed position.

Based on this, there is a trade-off between wear- and contact resistance when considering a composite material such as copper-tungsten. The effects of thermal stresses present during and after the making operation, must be taken into consideration when deciding the best material distribution. With a high tungsten density, the thermal stresses are lower during making operations than high copper density. While in the closed position, high tungsten density has higher thermal stress compared to high copper density.

In this master's thesis the main goal was to examine the contacts during making operation. Based on this, the best contact material is the one consisting of high tungsten density. However, as mention earlier, this is only one of four states a switching device can be in. High tungsten density might not be the best solution when examining open- , closed- and breaking operation.

6.3 Impacts Caused by the Short-Circuit Current and Arcing Time

In this master's thesis, one of the main aims were to examine the influence arcing time and short-circuit current had on the contact material, during making operation. Based on the equation for dissipated heat, by increasing either of them, the amount of dissipated heat increases.

From the results, when considering them separately it looks like arcing time was the most stressful. By increasing the arcing time, the contact was exposed for heat stresses for a longer period, increasing both the weld area and contact erosion. As previously mentioned, heat requires time to build up and distribute outwards in the contact material. At short arcing time, the accumulated heat was not high enough to cause evaporation of the contact surface. Causing low amounts of contact erosion and a weak arc weld.

It should be mentioned that the short-circuit current also had a large impact on the contacts. When considering a pre-strike arc with constant arcing time, the thermal stresses increases along with increasing short-circuit current.

From the simulations, the highest thermal stresses occurred at large short-circuit current (31.5 kA) and long arcing time (4 ms). Consequently, one of these should be reduced to decrease the amount of contact erosion and the arc weld strength. The arcing time is strongly dependent on the insulation medium, the short-circuit current and the contact material. While the short-circuit current strongly depends on the electrical components present in the electrical network. If possible, it is always preferable to decrease either current or arcing time in order to reduce the thermal stresses present during making and braking operations.

6.4 Validation of the Results

The COMSOL model created in this master's thesis has converted a complex making operation, to become a simplified model with low amounts of changing parameters. The model consists of inspiration from a variety of different pre-made modules that already was produced by the company COMSOL or by other skilful COMSOL users. For instance, the evaporation mechanism was created from a model simulating the heat shield on a spacecraft [23]. While the phase change mechanism was created from a model simulating ice melting, found in the application libraries in COMSOL. These modules increase the validity of the results, as they

were created by highly experienced people with a good understanding of the simulation program COMSOL.

The assumptions made in this master's thesis decreases the complexity of the simulated object. This was performed in order to simulate the influence pre-strike arcing had on the contact surface. All assumptions have been made with good intentions to not considerably influence the end results. A list of the assumptions were presented in section 4.10 *"Assumptions"*. Most likely, two of these assumptions reduced the validity of the results. These are the fifth assumption, considering the layered models compared with the cubical models, and the eighth assumption, not including a fuse mechanism into the model. However, these assumptions were made in order to create a working simulation. The original intention was to make a cubical model with a fusing mechanism, and it was tried implemented for a long period. However, this proved to be very difficult, based on the time frame of this master's thesis.

The layered model used, provides knowledge and supports what was previously presented in the theory about contact materials. Additionally, the model provides: a contact material that erodes when increasing above its vaporisation temperature, a contact material that changes its material properties when exceeding the melting temperature and a movement speed of the contacts. Hence, this supports the validity of the results.

Chapter 7

Conclusion

The work presented in this master's thesis examine the influence a pre-strike arc have on a medium voltage switching device during making operations. The objective were to find the amount of contact erosion and arc-weld strength after the making operation had occurred.

Three base models were developed in the simulation tool COMSOL Multiphysics. One for each contact material simulated: copper, tungsten and copper-tungsten. Each base model consisted of a fixed and a moving contact.

The contact surface were tested with different short-circuit currents and arcing times. The results showed that the contact consisting of pure copper generally had the lowest strength towards contact erosion and arc-welding. Additionally, copper-tungsten had the best toleration towards thermal stresses. This comes from the high wear strength of tungsten and the good thermal conductivity of copper, causing thermal stressed to be shared between the layers.

Based on the good capabilities of copper-tungsten, a simulation was developed to examine the impacts of different material distributions, i.e. high copper density and high tungsten density. Results implies that material distribution had a major impact on both the contact erosion and arc weld strength. By increasing the amount of tungsten, both contact erosion and arc weld strength decreased. This supports the theory, that an increase in tungsten reduces the contact wear of the contacts.

When examining copper-tungsten, it was observed that only copper particles melted and created an arc weld. This implies that the copper present had a substantial impact on the weld strength, i.e. increasing copper particles caused an increase in arc weld area.

Altogether, high tungsten density was the best contact material when examine the making operation. However, this is only one of four states a switching device can be in. A high tungsten density might not be the best solution when examining open- , closed- and breaking operation.

Chapter 8

Recommendations for Future Work

This master's thesis has utilized many of the possibilities that COMSOL has to offer. However, there is still some mechanisms that can be implemented in order to increase the validity of the simulations.

These measures are suggested for further works regarding the simulations of the contact surface of a switching device exposed for a pre-strike arc:

- Change the layered model into a cubical contact material. This could result in more valid values from the simulations of the contact material.
- Utilize an improved moving operation of the contacts, such that the movement does not influence the temperature distribution inside the contacts.
- Introduce a fluid flow and laminar flow inside the liquid material, to make it possible to simulate the welding mechanism of the contacts.

Chapter 9

Bibliography

[1]   Niayesh, K. and Runde, M. (2017). "Power Switching Components." [Trondheim]: Springer International Publishing.

[2]   Sanden, M. (2018). "Modelling of Electrical Contact Behaviour Using COMSOL", Specialisation project

[3]   Shea, J. (1999). "Erosion and resistance characteristics of AgW and AgC contacts." IEEE Transactions on Components and Packaging Technologies, 22(2), pp.331-336.

[4]   J. J. Shea, "High Current AC Break Arc Contact Erosion," 2008 Proceedings of the 54th IEEE Holm Conference on Electrical Contacts, Orlando, FL, 2008, pp. xxii-xlvi.

[5]   Contact Technologies. (2018). "Contact Material Selection." [online] Available at: http://www.contactechnologies.com/Contact-Technologies-Materials.html [Accessed 4 Dec. 2018].

[6]   Zhu, D., Wu, H., Yuan Chang, Y. and Kuang, K. (2018). "Process For Making Copper Tungsten And Copper Molybdenum Composite Electronic Packaging Materials." [online] Freepatentsonline.com. Available at: http://www.freepatentsonline.com/20100092327.pdf [Accessed 4 Dec. 2018].

[7]   M. Mohammadhosein, K. Niayesh, A.A.S. Akmal, H. Mohseni, "Impact of Surface Morphology on Arcing Induced Erosion of CuW Contacts in Gas Circuit Breakers" 2018 Holm Conference on Electrical Contacts, Albuquerque, NM,2018 pp.1-7.

[8]   Chemistry LibreTexts. (2018). "Heat of Sublimation". [online] Available at:
        https://chem.libretexts.org/Bookshelves/Physical_and_Theoretical_Chemistry_Textbook_Maps/Sup
        plemental_Modules_(Physical_and_Theoretical_Chemistry)/Thermodynamics/Energies_and_Potent
        ials/Enthalpy/Heat_of_Sublimation# [Accessed 21 jun. 2019].

[9]   P.G. Slade, "Electrical Contacts Principles and Applications, second edition," 2013.

[10]   E. Ildstad, "Compendium - TET4160 Insulating Materials for High Voltage Application" 2017,
        NTNU.

[11]   Niemeyer, L., Ullrich, L. and Wiegart, N. (1989). "The mechanism of leader breakdown in
        electronegative gases." *IEEE Transactions on Electrical Insulation*, 24(2), pp.309-324.

[12]   G. Sandolache and S. W. Rowe, "Vacuum Breakdown between Molten Metal Electrodes," 2006
        International Symposium on Discharges and Electrical Insulation in Vacuum, Matsue, 2006, pp. 13-
        16.

[13]   COMSOL, "COMSOL Multiphysics User's Guide." Version 4.3, May 2012. Chapter 13, 18 and 19.

[14]   Chekhovskoi, V., Tarasov, V. and Gusev, Y. (2000). "Calorific properties of liquid copper." *High
        Temperature*, 38(3), pp.394-399.

[15]   David R. Lide, ed., "CRC Handbook of Chemistry and Physics." Internet Version 2005,
        <http://www.hbcpnetbase.com>, CRC Press, Boca Raton, FL, 2005.

[16]   Giordanengo, B., Benazzi, N., Vinckel, J., Gasser, J. and Roubi, L. (1999). "Thermal conductivity
        of liquid metals and metallic alloys." *Journal of Non-Crystalline Solids*, 250-252, pp.377-383.

[17]   Tolias, P. (2017). "Analytical expressions for thermophysical properties of solid and liquid tungsten
        relevant for fusion applications." *Nuclear Materials and Energy*, 13, pp.42-57.

[18]   Paradis, P., Ishikawa, T. and Yoda, S. (2005). "Viscosity of liquid undercooled tungsten." *Journal
        of Applied Physics*, 97(10), p.106101.

[19]   Hixson, R. and Winkler, M. (1990). "Thermophysical properties of solid and liquid tungsten."
        International Journal for Thermosphysics, 11(4), pp.709-718.

[20]   Battezzati, L. and Greer, A. (1989). "The viscosity of liquid metals and alloys." *Acta Metallurgica*,
        37(7), pp.1791-1802.

[21]   Hust, J., Hust, J. and Lankford, A. (1984). "Thermal conductivity of aluminum, copper, iron, and
        tungsten for temperatures from 1 K to the melting point." 1st ed. Colorado: U.S. Department of
        Commerce Boulder.

[22]   Konstantinova, N., Popel', P. and Yagodin, D. (2009). "The kinematic viscosity of liquid copper-aluminium alloys". *High Temperature*, 47(3), pp.336-341.

[23]   Frei, W. (2016). "Modeling Thermal Ablation for Material Removal." [online] COMSOL Multiphysics. Available at: https://www.comsol.com/blogs/modeling-thermal-ablation-for-material-removal/ [Accessed 10 Jun. 2019].

[24]   Matweb.com. (2019). "Copper, Cu; Annealed." [online] Available at: http://www.matweb.com/search/datasheet_print.aspx?matguid=9aebe83845c04c1db5126fada6f76f7e [Accessed 10 Jun. 2019].

[25]   Matweb.com. (2019). "Tungsten, W." [online] Available at: http://www.matweb.com/search/datasheet_print.aspx?matguid=41e0851d2f3c417ba69ea0188fa570e3 [Accessed 10 Jun. 2019].

[26]   M. Kim, K. Kim, A. Smajkic, M. Kapetanovic and M. Muratovic, "Influence of contact erosion on the state of SF6 gas in interrupter chambers of HV SF6 circuit breakers," 2014 IEEE   International Power Modulator and High Voltage Conference (IPMHVC), Santa Fe, NM, 2014, pp. 466-469.

[27]   E. Walczuk, "Arc Erosion of High Current Contacts in the Aspect of CAD of Switching Devices," 38th IEEE Holm Conference Proceedings, pp. 1-16, 1992.

[28]   Tepper, J., Seeger, M., Votteler, T., Behrens, V. and Honig, T. (2006). «Investigation on Erosion of Cu/W Contacts in High-Voltage Circuit Breakers." *IEEE Transactions on Components and Packaging Technologies*, 29(3), pp.658-665.